1-1-2008

Design of a cyclic pressure bioreactor for the ex vivo study of aortic heart valve mechanobiology

Kimberly Jo Schipke

DESIGN OF A CYCLIC PRESSURE BIOREACTOR FOR THE *EX VIVO* STUDY OF AORTIC HEART VALVE MECHANOBIOLOGY

By

Kimberly Jo Schipke

A Thesis
Submitted to the Faculty of
Mississippi State University
in Partial Fulfillment of the Requirements
for the Degree of Master of Science
in Biomedical Engineering
in the Department of Agricultural and Biological Engineering

Mississippi State, Mississippi

August 2008

DESIGN OF A CYCLIC PRESSURE BIOREACTOR FOR THE *EX VIVO*

STUDY OF AORTIC HEART VALVE MECHANOBIOLOGY

By

Kimberly Jo Schipke

Approved:

_____	_____
Steven Elder Associate Professor of Agricultural and Biological Engineering (Director of Thesis)	James N. Warnock Assistant Professor of Agricultural and Biological Engineering (Major Professor)
_____	_____
Carl McCoy Professor of College of Veterinary Medicine Pathobiology/Population Medical Department (Committee Member)	Jun Liao Assistant Professor of Agricultural and Biological Engineering (Committee Member)

_____

Sarah Rajala
Dean of the College of Engineering

Name: Kimberly Jo Schipke

Date of Degree: August 9, 2008

Institution: Mississippi State University

Major Field: Biomedical Engineering

Thesis Director: Dr. Steven Elder

Major Professor: Dr. James N. Warnock

Title of Study: DESIGN OF A CYCLIC PRESSURE BIOREACTOR FOR THE *EX VIVO* STUDY OF AORTIC HEART VALVE MECHANOBIOLOGY

Pages in study: 87

Candidate for Degree of Master of Science

The differentiation of myosin into the respective heavy chain isoforms has shown a correlation with high mechanical stress. Aortic valve myosin expression has been reported; however, the characterization of the pressure response has yet to be fully developed. Thus, a cyclic pressure bioreactor was developed to elucidate the α/β-myosin heavy chain (MHC) expression in aortic valve leaflets subject to physiological and pathological transvalvular pressure loads. The pressure bioreactor achieved the desired pressure modulation via LabVIEW controlled solenoid valves. Results showed α/β-MHC expression on the fibrosal endothelium and minimal dispersal in the subendothelium, indicating the presence of smooth muscle cells. Endothelial layer denudation was evident with time progression while protein expression was limited to sites of excision or injury, indicating a causal relationship with high shear stress. In conclusion, α/β-

MHC expression is limited by endothelium detachment and lack of smooth muscle cells, possibly on account of insufficient mechanical stimuli.

DEDICATION

I would like to dedicate this research to my parents, Dwight and Shelley Schipke, grandmother, Joanne Mutchler, sister, Shauna Hutton, and brothers, Shad and Brad Schipke, for their endless inspiration and encouragement. They have supported all my decisions in life and helped mold me into the person I am today. I am very grateful for the loving roles they have played in my life.

ACKNOWLEDGMENTS

The author expresses her sincere gratitude to those who have put forth time and energy into the materialization of this thesis. First of all, the author would like to thank Dr. James Warnock for his guidance and support throughout this research project. Expressed appreciation is also due to the other members of the thesis committee, namely, Dr. Steven Elder, Dr. Jun Liao, and Dr. Carl McCoy, for their direction and input. A debt of gratitude is due to Dr. Filip To for helping me with the computer programming and troubleshooting needed for this study. Shad Schipke should also be recognized for his insight on the initial pressure chamber design. Lastly, the author would like to extend much thanks to Scott Metzler for his assistance, input, support, and continual inspiration.

TABLE OF CONTENTS

DEDICATION ii

ACKNOWLEDGMENTS iii

LIST OF TABLES vi

LIST OF FIGURES vii

CHAPTER

I. INTRODUCTION 1

Cardiovascular Disease 2
Aortic Valve Physiology 3
Aortic Valve Cellular Biology 7
Endothelial Cells 8
Interstitial Cells 9
Aortic Valve Biomechanics 13
Hypertension 19
Aortic Valve Disease 20
Aortic Stenosis 21
Aortic Regurgitation 21
Current Treatment Options 22
Bioprosthetic Aortic Valves 22
Mechanical Aortic Valves 24
Tissue Engineered Aortic Valves 25
Objective of the Study 27
Scope and Limitations of the Study 28

II. DESIGN OF A CYCLIC PRESSURE BIOREACTOR 29

Brief History of Heart Valve Bioreactors 29
Design Requirements 30
System Overview 31
Materials 32

Pressure Chamber Materials 32
Electrical Devices Used 34
Procedure Used to Run Bioreactor 35
Sterility Tests 36
Results 36
Discussion 39

III. PRELIMINARY STUDY OF α/β-MYOSIN EXPRESSION 44

Introduction 44
Methods 45
Results 47
Discussion 54
Summary 57

BIBLIOGRAPHY 58

APPENDIX

A. SOLIDWORKS DRAWINGS OF BIOREACTOR 70

Isometric View of Bioreactor with Material Properties 71
Dimensions of Front End Plate 72
Dimensions of Rear End Plate 73
Dimensions of Acrylic Cylinder 74
Dimensions of Sample Plate 75
Dissected Side View of Bioreactor 76
Front View of Bioreactor 77
Top View of Bioreactor 77

B. ACTUAL PHOTOGRAPHS OF PRESSURE CHAMBER SYSTEM 78

Bioreactor within Incubator 79
Top View of Bioreactor with Circuit Board 79

C. SCHEMATIC DRAWING OF ELECTRICAL CIRCUITRY 80

D. LABVIEW USER INTERFACE 82

E. PROTOCOLS 84

Aortic Valve Leaflet Extraction and Culture 84
Immunohistochemisty Protocol for TRS/Proteinase K Pretreatments 85

LIST OF TABLES

1. Interstitial cell classification via contractile protein antigen reaction..... 11

2. Classification of blood pressure 19

LIST OF FIGURES

1. Schematic diagram of the trilayer configuration of an aortic valve, illustrating the elastin sheets within the ventricularis, GAG-rich matrix comprising the spongiosa, and the collagen fibers contained within the fibrosa 5

2. Masson's trichrome stain of collagen (blue) within the (A) fibrosa and (B) ventricularis 6

3. Aerial view of aortic valve indicating alignment conventions in the radial (R) and circumferential (C) direction 7

4. Illustration of the line of coaptation 14

5. Demonstration of collagen alignment when radially and biaxially stretched 15

6. Typical plot of leaflet length vs. pressure gradient across the leaflet in vivo in a single dog. The circles represent measured leaflet length and measured pressure gradient in diastole. The bars represent measured leaflet length and assumed pressure gradient of 0 to 10mmHg in systole. The lengths ℓ_0, ℓ, ℓ_1, and ℓ_2 correspond to the gradients of 0, 10, 60, and 200mmHg, respectively. Diastolic strain is represented by ε_D, whereas systolic strain is represented by ε_S 18

7. (A) Allograft (B) Porcine xenograft bioprosthetic valve 24

8. Mechanical valves (A) Starr-Edwards caged ball (baxter.com) (B) Sorin Medical tilting disk (sorin.com) (C) St. Jude's bileaflet (sjm.com).. 25

9. Schematic of operation of normally-closed viton diaphragm solenoid valve 33

10. Graph of pressure simulation within bioreactor at (A) normotensive, (B) Stage I hypertensive, and (C) Stage II hypertensive conditions 38

11. Immunohistochemistry of α/β-myosin heavy chain of leaflet fixed immediately after excision (A) 10x (B) 40x (focused on endothelium) 48

12. Immunohistochemistry of α/β-myosin heavy chain of leaflet fixed immediately after excision (A) 10x (B) 40x (focused on spongiosa layer)..... 49

13. Immunohistochemistry of α/β-Myosin heavy chain after 24 hours in media (A) 10x (B) 40x (focused on fibrosal endothelium and spongiosa) 50

14. Immunohistochemistry of α/β-Myosin heavy chain exposed to 40-80mm Hg cyclic pressure (A) 10x (B) 40x (focused on site of excision)... 51

15. Immunohistochemistry of α/β-Myosin heavy chain exposed to 40-90mm Hg cyclic pressure (A) 10x (B) 40x (focused on site of excision)... 52

16. Immunohistochemistry of α/β-Myosin heavy chain exposed to 40-100mmHg cyclic pressure (A) 10x (B) 40x (focused on fibrosal endothelium). 53

CHAPTER I

INTRODUCTION

The aortic valve is located between the left ventricle and the aorta, and allows unidirectional blood flow, preventing backflow into the ventricle. The valve withstands a harsh, dynamic environment that is constantly exposed to several different types of mechanical stresses, including shear, bending, tension, and compression. Aortic valve disease (AVD) is a form of cardiovascular disease that results in either restricted blood flow across the valve, or regurgitation of blood into the left ventricle. Symptoms associated with AVD include shortness of breath, angina, dizziness, heart palpitation, etc., which are symptoms similar to several other cardiovascular diseases; therefore, AVD is difficult to detect until valve replacement and surgical intervention are necessary. Current treatment options include the use of mechanical or prosthetic valves, capable of functioning effectively for approximately ten years. While suitable for adults, children with malfunctioning valves must undergo repeat operations as artificial valves are unable to grow with the child. Improved understanding of valve mechanobiology in response to pressure would help elucidate the mechanisms of valve pathogenesis. In turn, this could help in the development of non-invasive therapies such as pharmaceutical prevention. This thesis aims to explore the

aortic valve's response to cyclic transvalvular pressure, with respect to α/β-myosin heavy chain expression, to give further insight into the appearance of muscle fibers in a normally passive valve.

Cardiovascular Disease

Cardiovascular disease (CVD) is the leading cause of death and accounts for approximately 30% of all deaths worldwide. In 2005, an estimated 17.5 million people died from cardiovascular diseases, which include coronary heart disease, hypertension, aortic valve disease (AVD), rheumatic heart disease, congenital heart disease, and heart failure. [1] In the United States today, approximately 80,700,000 adults are diagnosed with one or more types of CVD. Every 37 seconds an American dies of CVD; this amounts to almost 2,400 deaths each day. [2] Furthermore, an estimated $448.5 billion will be spent on the direct and indirect costs of CVD in the U.S. in 2008. [2]

Several CVDs are correlated with different aortic valve pathologies, due to the importance of maintaining physiological valve contraction and subsequent ventricular ejection. Aortic valve disease may be caused by congenital valve disease, infective endocarditis, rheumatic fever, fibro-calcific degeneration, or possibly dilation of the valve annulus, amongst others. [2-5] In 2002, over 12,500 American deaths were directly attributed to aortic valve disease. AVD was also an underlying factor in an additional 26,336 deaths and 48,000 hospital discharges. [6]

Aortic Valve Physiology

Aortic valve leaflets are composed of interstitial cells suspended within an extracellular matrix and are lined with an endothelial cell monolayer. The extracellular matrix (ECM) within the valve is composed of hyaluronic acid, proteoglycans, glycosaminoglycans, and collagen fibrils, which bear the majority of the tensile and compressive forces acting on the leaflet. [7,8] The collagenous tissue of the valve is composed of ~60-70% water by weight, which is tightly bound to the fibrous tissue network and contributes to valve incompressibility. Leaflets exhibit viscoelastic behavior due to the elastic response to loading from the solid ECM components, and a viscous response attributed to the fluid components. The aortic valve is composed of three layers: the fibrosa, located on the aortic surface of the valve; the spongiosa, the middle layer; and ventricularis, found on the ventricular side of the valve. A schematic diagram of the organization of the structural components of an aortic valve leaflet can be seen in **Figure 1**, whereas actual collagen composition can be seen via Masson's trichrome stain in **Figure 2**. The structure of each layer plays a critical role in the maintenance and operation of the valve. [9-12]

Aortic valve leaflets exhibit significant directionality of structural components. The specific alignment of fibrous components lends the valve its highly anisotropic strain response. [7,13,14] The orientation of aortic valve components can be characterized as either radially or circumferentially aligned and is depicted in **Figure 3**. The radial direction describes the alignment along the

leaflet from the aortic root attachment extending out toward the tricuspid nexus of the aortic valve. The circumferential direction indicates that the alignment follows the imaginary perimeter of the valve annulus ring and decreasing concentric circles that span the three leaflets.

The mechanical properties of the aortic valve are supplied by only the fibrosa and ventricularis layers. Collagen and elastin are the principal structural components of heart valves. The fibrosa is composed mainly of collagen and constitutes 30-40% of the total thickness of the valve. [15] The fibrosal collagen, organized into fibers and bundles, is predominantly circumferentially aligned. Collagen within the ventricularis is less prevalent and more disordered, as compared to collagen within the fibrosa. The ventricularis combines collagen with elastin fibers, which are organized into a mesh, or continuous sheet that spans the entirety of the layer. [16] Elastin located within the fibrosa is more sporadic, manifesting in large tubes of loose mesh that surround the much larger collagen bundles, aligned circumferentially.

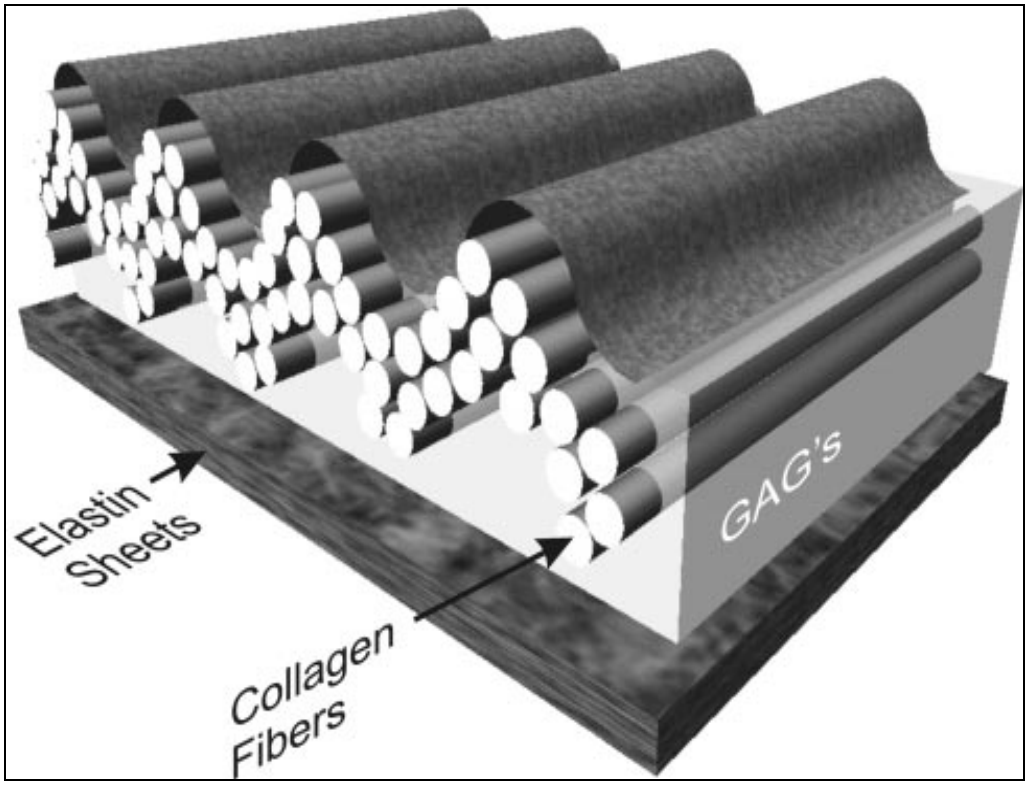

Figure 1: Schematic diagram of the trilayer configuration of an aortic valve, illustrating the elastin sheets within the ventricularis, GAG-rich matrix comprising the spongiosa, and the collagen fibers contained within the fibrosa.

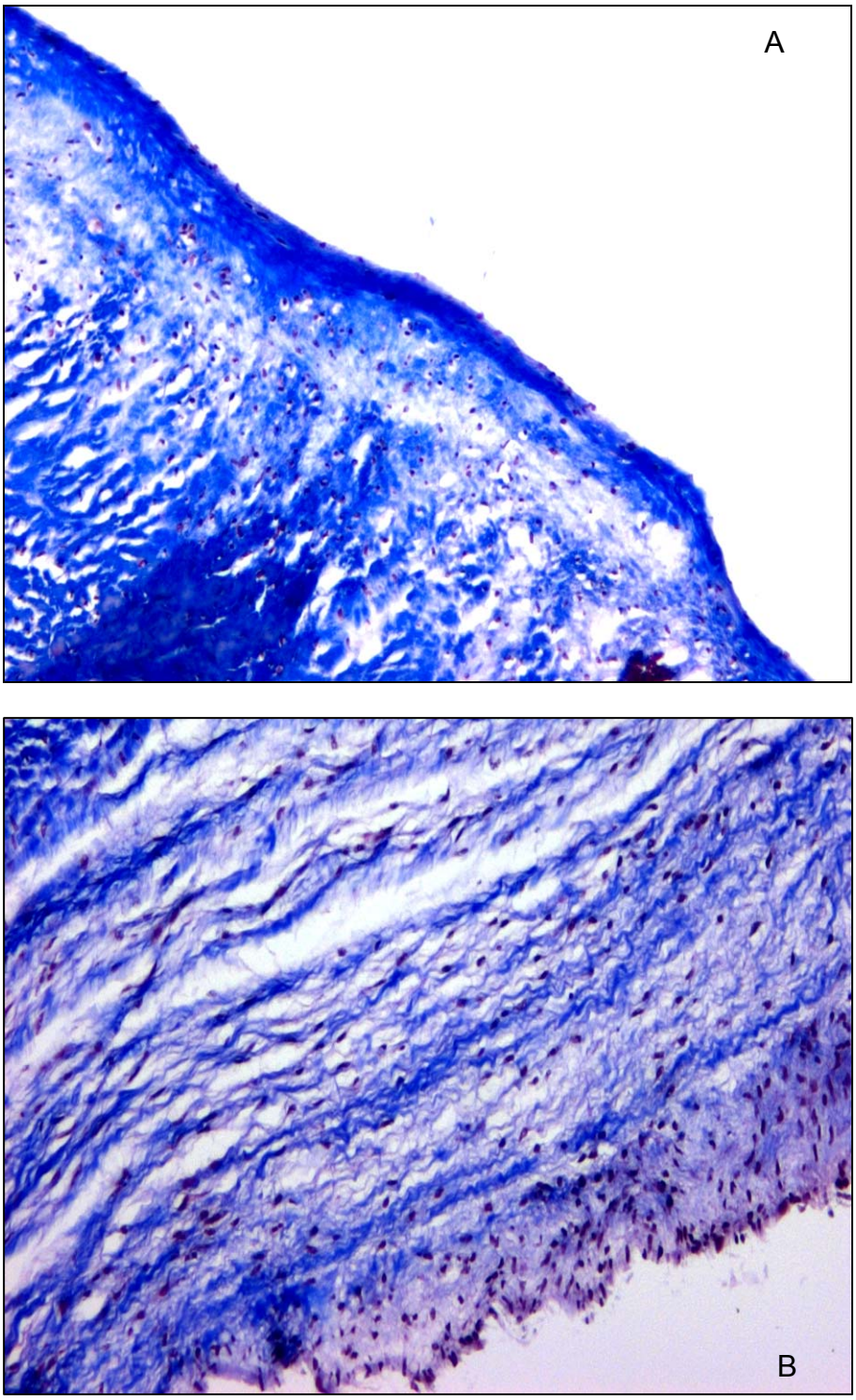

Figure 2: Masson's trichrome stain of collagen (blue) within the (A) fibrosa and (B) ventricularis

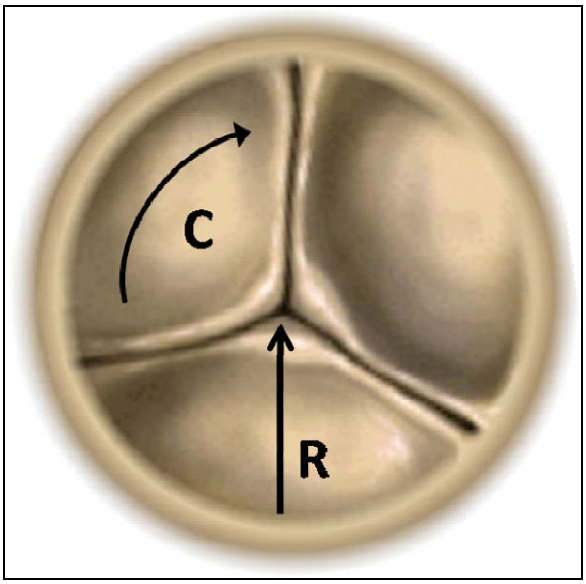

Figure 3: Aerial view of aortic valve indicating alignment conventions in the radial (R) and circumferential (C) direction

Aortic Valve Cellular Biology

The mature aortic valve functions through complex interactions between two distinct cell types, the endothelial cells and the interstitial cells. To fully appreciate the individual cell phenotypes, a brief overview of the origins of the cell types and the valve maturation process, known as valvulogenesis, is needed. The embryonic heart begins as a primitive bi-layered tube of adjacent endocardial and myocardial monolayers encompassing an interstitial matrix known as cardiac jelly. As the heart develops further, the cells and jelly that cover the future atrioventricular canal and outflow tract begin to distend outward. The resulting protrusions are referred to as cardiac cushions. [17] A process known as the endothelial to mesenchymal transformation, or EMT, occurs which results

in delamination and remodeling events. While the atrioventricular tract cushions eventually form the mitral and tricuspid valves, the aortic valve forms in the developmental outflow tract. The exact pathways that lead to the differentiation are not currently known, although intense research has been focused on the role of growth factors, endothelial nitric oxide synthase, and bone morphogenic proteins, matrix metalloproteases, periostin, etc. [18-22] The end stage functional aortic valve leaftlet has recently been shown to have cell populations with an endothelial origin. [23,24] A key tenet of aortic valve cellular biology is the plasticity of the cell phenotypes, which allows for extensive remodeling essential to valve durability.

Endothelial Cells

The aortic valve endothelial cell is an extremely mechanosensitive cell type. The aortic valvular endothelial cell senses a variety of forces *in vivo*, including fluid shear stress due to the demanding pulsatile hemodynamic environment, and cyclic strain with particular regard to diastolic transvalvular pressure. Endothelial cells have a cobblestone-like morphology and readily form monolayers on both sides of the valve leaflet. The endothelial cell is circumferentially aligned on both sides of the aortic valve. [25] A key function of the endothelial layer is to sense environmental forces and transmit biochemical signals to the interstitial cells. [26] Aortic valve sclerosis has been linked to an initial event of endothelial layer removal, or denudation. A pro-inflammatory reaction occurs, which allows endothelial cells to produce adhesion molecules to bind

circulating leukocytes and allow migration into the sub-endothelial layer. [27] Current research is being conducted to further elucidate the mechanobiology of the valvular endothelial cell.

Valvular endothelial cells are a distinct cell population from the vascular endothelial cell. J. Butcher observed the rearrangement of focal adhesions to regulate the directional response to shear stress. The vascular endothelial cell aligns parallel to the direction of flow, whereas the valvular endothelial cell aligns perpendicularly to the direction of flow. [28,29] It is not currently known whether the fibrosal endothelial cell is a distinct phenotype from the ventricularis endothelial cell, although gene expression profiles have indicated they may be different. [30] The response of endothelial cells to other mechanical stimuli, such as stretch and pressure, are currently under investigation.

Interstitial Cells

As previously stated, interstitial cells respond to mechanical stimuli as well as biochemical signals transmitted from endothelial cells. Studies have shown that interstitial cells are responsible for repairing and remodeling the valve leaflets by increased cell proliferation, migration, and matrix synthesis or degradation, depending on the biochemical signaling or intensity of mechanical stimuli. [31] Three distinct phenotypes of interstitial cells have been characterized in the mature native valve: fibroblasts, myofibroblasts, and smooth muscle cells. [32] About 80% of interstitial cells in normal, non-collagen synthesizing cells have been classified as quiescent fibroblasts and are characterized by vimentin

expression, but these fibroblasts do not express α-smooth muscle actin, or non-muscle myosin heavy chain. [33,34] However, while actively remodeling the valve, fibroblasts synthesize collagen, elastin, proteoglycans, growth factors, cytokines, fibronectin, chemokines, and matrix metalloproteinases (MMPs). Valvular metalloproteinases perform extracellular matrix remodeling and control growth factor production. [35] Fibroblasts have been shown to differentiate into myofibroblasts when stimulated by transforming growth factor-β, as a result of increased contractility and up-regulation of extracellular protein production in transdifferentiated cells. [36]

The dynamic, myofibroblast phenotype has been shown to differentiate between fibroblast and smooth muscle cell, and is also suggested to be involved in cellular contraction, proliferation, and migration. Myofibroblasts display characteristics of both fibroblasts and smooth muscle cells by expressing contractile properties, secreting extracellular matrix, and containing both muscle and non-muscle regulatory and structural proteins. [37,38] Myofibroblasts are typically characterized by antibody reactions to microfilaments (α-smooth muscle actin) and intermediate filaments (vimentin and desmin). [9]

Smooth muscle cells, the third interstitial cell phenotype, have been found either singly or arranged in thin bundles and are also thought to be involved in valvular contraction. [39] Smooth muscle cells are distinguished by the expression of α/β-myosin heavy chain, SM1, representing differentiated smooth muscle cells; and by the expression of α-myosin heavy chain, SM2, representing mature

smooth muscle cells. Rabkin et al. has shown that the phenotypic state of valvular interstitial cells is related to the remodeling demand of the tissue, and has correlated cellular contractility to biosynthetic activity. [40] To support this claim, Merryman et al. has shown a strong relationship between smooth muscle actin and HSP47, a collagen biosynthetic protein. The results of Merryman's study imply that homeostasis is continually maintained by valve remodeling via collagen production and phenotypic differentiation from fibroblasts into myofibroblasts and smooth muscle cells. [41]

As previously stated, several different types of contractile proteins are found within the aortic valve. Various antibodies for contractile proteins, such as vimentin, α-actin, and myosin, have been used to characterize valvular interstitial cells into fibroblasts, myofibroblasts, and smooth muscle cells. **Table 1** illustrates interstitial cell reaction to contractile antibodies. Endothelial cells stain heavily for vimentin; however, no studies have shown positive staining for desmin or α-smooth muscle actin. Myosin has been found within the endothelial layer, but the exact form of myosin has yet to be classified. [42]

Table 1: Interstitial cell classification via contractile protein antigen reaction [9]

Antibody	Filament System	Fibroblasts	Myofibroblasts	SMC
Vimentin	Intermediate-mesenchymal	+	+	+/-
α-Actin	Microfilament-actin	-	+/-	+
SM1	α/β-Myosin heavy chain	-	+/-	+
SM2	α-Myosin heavy chain	-	+/-	+

Vimentin is an intermediate filament protein and is the first protein to be expressed during cell differentiation. During valvulogenesis, vimentin has been shown to align circumferentially on the ventricularis, whereas it appears as a network on the fibrosa. [43] Additionally, valvular endothelial cells have a higher volume density of vimentin as compared to valvular interstitial cells, suggesting an accommodative mechanism involving such filaments. [44] Although classified as a cytoskeletal protein, vimentin has also proven available for autoantibody binding and T-cell recognition; therefore, vimentin may be involved in the inflammation of the heart as with rheumatic heart disease. [45]

α-Smooth muscle actin (α-SMA) is a microfilament found within cells that require migration. Interstitial cell fibroblasts are quiescent; however, when cellular migration is necessary, they differentiate into myofibroblasts (and sometimes smooth muscle cells) and acquire α-SMA for locomotion. [34] For this reason, α-SMA is often used as a myofibroblast marker. Migration may be required for tonus in response to mechanical stimuli, or possibly as an immune response to injury. During embryonic development, α-SMA is scarce on both faces of the valve cusps but is suspected to increase after the initiation of interstitial cell differentiation. [43]

Myosin heavy chain (MHC) is found as three different dimers: (1) two α-MHC form a homodimer; (2) one α- and one β-MHC form a heterodimer; and (3) two β-MHC form a homodimer. [46-48] These dimers are characterized by Ca^{2}-

activated ATPase activity and mobility, with α-MHC having the most contractility and β-MHC having the least. [48] β-MHC and α-MHC are characterized as slow- and fast-twitch muscle fibers, respectively. α/β-MHCs, consequently, show characteristics of both α-MHC and β-MHCs and are thus believed to be an intermediate form of MHC. β-MHCs are exclusively found in embryonic heart development and are eventually completely replaced by α-MHCs in an adult. [47] Studies have shown adult α-MHC in the heart redifferentiates into β-MHC as a result of increases in mechanical stimuli for extended periods of time, as with hypertrophy; however, as mechanical stimuli decrease in intensity, β-MHC reverts to α-MHC. [47,49,50] Interestingly, research shows no α-MHC is present in the end-stage failing human heart, which may suggest full redifferentiation to developmental slow-twitch β-MHC unable to meet functioning heart contraction. [51] Also, weakened, enlarged hearts, a condition known as dilated cardiomyopathy, is also associated with increased β-MHC and a decreased contractility. [52] To date, valve research has found α/β-MHC and α-MHC in smooth muscle cells within remodeling valves; however, β-MHC expression within heart valves has been ignored and should be investigated further.

Aortic Valve Biomechanics

Located between the left ventricle and aorta, the aortic valve allows blood passage in systole, and prevents retrograde blood flow during diastole. The three valve cusps open in the systolic phase with maximum flexibility and close in the diastolic phase with necessary tissue strength. The aortic valve changes

geometry throughout the cardiac cycle in response to loading. The cusps rotate when opening and closing, which causes a bending stress along the line of coaptation, located radially from the area of leaflet attachment. [53] The location of the line of coaptation is illustrated in **Figure 4**. Collagen within the fibrosa layer allows for maximum leaflet coaptation during closure and plays a vital role in maintaining valve durability. During systole, collagen fibers in the fibrosa layer become folded and compacted to allow for maximum orifice area for blood flow. Alternatively, during diastole when the valve is closed and under tensile stress, the collagen fibers are uncrimped and reoriented to withstand high mechanical stress. [9,54]

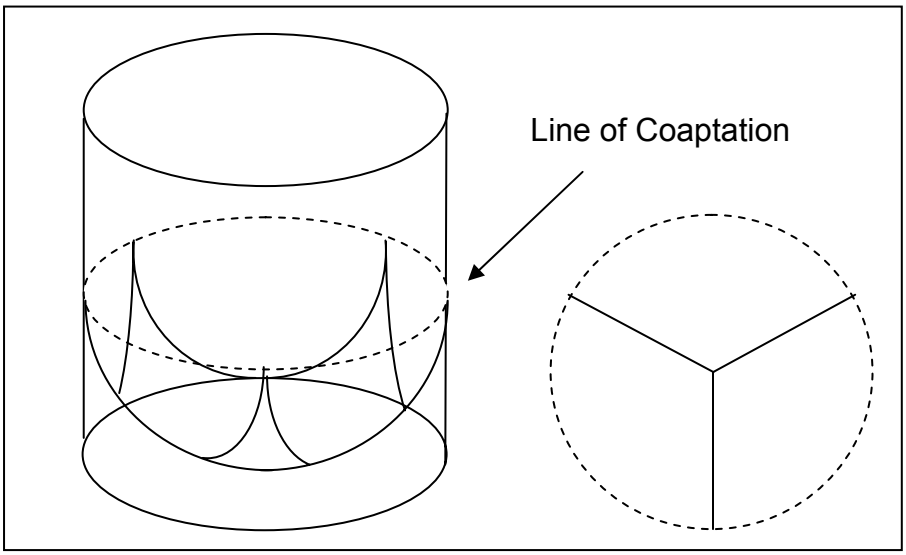

Figure 4: Illustration of the line of coaptation

The spongiosa layer contains hydrophilic proteoglycans which are responsible for cushioning and absorbing stress. [9,54] The elastin in the

ventricularis layer serves to maintain the circumferential alignment and proper spacing of collagen bundles when the valve is open during systole. Elastin provides the recoil necessary to properly align the fibers when the leaflets begin to close and extend out toward the line of coaptation. [9,54,55] Vesely and Noseworthy found that the amounts of collagen within the radially-oriented ventricularis and fibrosa are similar, but the fibrosa has higher radial extensibility due to its highly folded configuration. [55,56] Aortic leaflets under tensile stress have shown a significant difference in stiffness in the circumferential direction as compared to the radial direction. [57] As a result, circumferentially aligned collagen fibers in tension prevent separation of radially aligned collagen fibers, illustrated in **Figure 5**. [58]

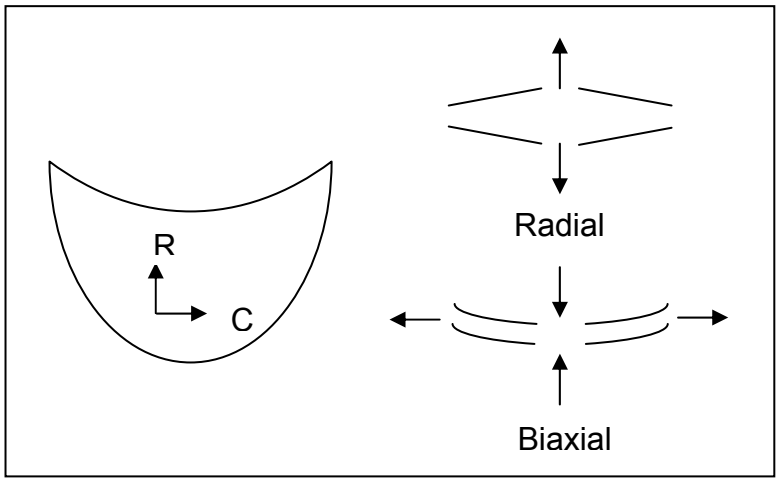

Figure 5: Demonstration of collagen alignment when radially and biaxially stretched [58]

The transvalvular pressure gradient dictates the opening and closing of the aortic valve. The valve is closed until ventricular pressure surpasses aortic pressure, at which point the aortic valve opens and releases the pressure across the valve. Pressure levels in the aorta vary from 80-120mmHg, affecting the fibrosa layer of the aortic valve; whereas, pressure levels in the left ventricle vary from 0-120mmHg, affecting the ventricularis layer. For this reason, the valve is constantly exposed to transvalvular pressure gradients ranging from zero when the valve is open, up to 80mmHg when the valve is closed in normal conditions. Studies show that valvular cells from the left side of the heart are stiffer when compared to valvular cells from the right side of the heart, which correlates with the higher transvalvular pressure experienced by the left side (when compared to the right side) of the heart. [41] In addition, α-smooth muscle actin content and collagen biosynthesis were also correlated to cellular stiffness and transvalvular pressure. Elevated pressures result in increased bending stresses and leaflet strains, which are also correlated to collagen biosynthesis. [41] Thubrikar et al. modeled *in vivo* leaflet stress as a function of transvalvular pressure by considering bending and stretching independently:

$$Stress = \left(\frac{PR}{T}\right) \pm E\left(\frac{T}{2R}\right)$$

where P represents transvalvular pressure, R denotes the radius of the leaflet, T is valve thickness, and E is the leaflet modulus of elasticity. The bending stresses affecting the valve are either tensile (+) or compressive (-), depending

on the side of the leaflet. [13] Diastolic leaflet strain, ε_D, as a result of transvalvular pressure can be calculated experimentally, using the following equation:

$$\varepsilon_D = \ell_2 - \ell_1 / \ell_1$$

where ℓ_2 represents the radial length of the leaflet at the highest transvalvular pressure gradient, and ℓ_1 corresponds to radial leaflet length at a 60mmHg pressure gradient. **Figure 6** demonstrates how diastolic strain can be calculated experimentally.

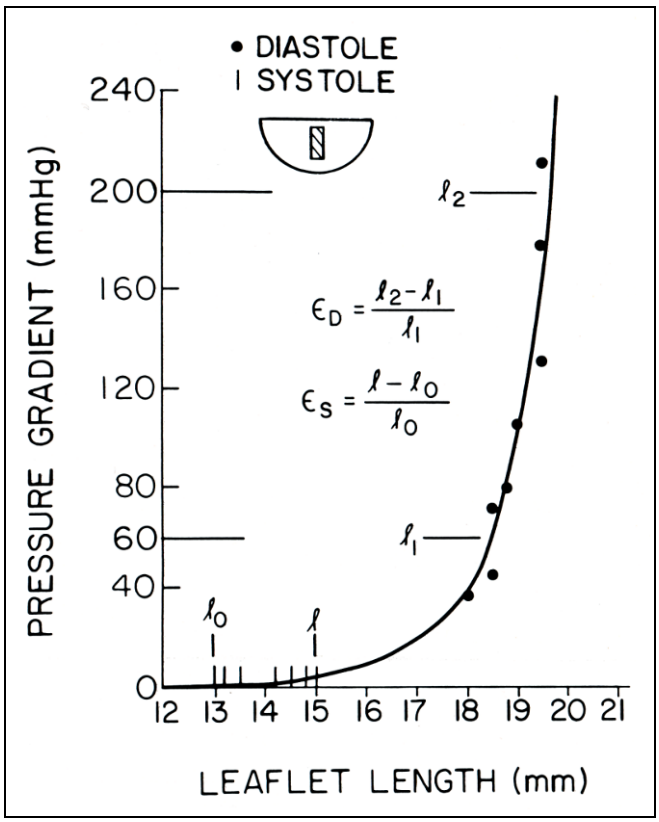

Figure 6: Typical plot of leaflet length vs. pressure gradient across the leaflet *in vivo* in a single dog. The circles represent measured leaflet length and measured pressure gradient in diastole. The bars represent measured leaflet length and assumed pressure gradient of 0 to 10mmHg in systole. The lengths ℓ_0, ℓ, ℓ_1, and ℓ_2 correspond to the gradients of 0, 10, 60, and 200mmHg, respectively. Diastolic strain is represented by ε_D, whereas systolic strain is represented by ε_S. [58]

Research has shown calcific lesions in diseased valves tend to occur in areas of high mechanical stress as a result of endothelial disruption or interstitial matrix damage. [59-61] Moreover, calcified sclerotic lesions typically occur in the subendothelial space on the aortic side of the valve (fibrosa) in regions of low shear stress with oscillatory flow. [62,63] Calcific deposits are also common along

the line of coaptation as a result of high bending stress. [61] These studies prove that mechanical stresses play a significant role in valvular pathogenesis. Further investigation of the biological response to force will broaden the working knowledge of heart valve biomechanics and associated diseases.

Hypertension

Elevated blood pressure alters the mechanical environment of the aortic valve and has been linked to aortic valve disease. According to the American Heart Association, nearly one in three adults in the United States is diagnosed with high blood pressure. [2,53] Hypertension is a risk factor for several cardiovascular disorders, including heart failure, stroke, atherosclerosis, intracranial hemorrhage, and dissecting aortic aneurysms. In 2004, high blood pressure total mention mortality was around 300,000 which is a 56.1% increase in deaths since 1994. [2,53] Hypertension is defined as a persistent elevation of blood pressure and is classified by the criteria shown in **Table 2**. [64]

Table 2: Classification of blood pressure

	Diastolic (mmHg)	Systolic (mmHg)
Normotensive	< 80	<120
High Blood Pressure	80-89	120-139
Stage I	90-99	140-159
Stage II	100-109	160-179
Stage III	110-119	180-209
Stage IV	>120	>210

Hypertension may be a result of abnormal functioning of the kidneys, heart, vasculature, or nervous system, improper diet, genetics, or a combination thereof. [65-67] For example, excessive renin secretion by the kidneys and the associated increase in water and sodium retention can elevate blood pressure. When hypertension is a result of another disorder (i.e. kidney disease), it is referred to as secondary hypertension; whereas, when the exact cause is unknown, it is referred to as primary hypertension. High blood pressure is either induced by, or causes, functional and morphological changes in the vasculature, such as thickening of the arterial wall and altered stiffness and contractile response. Similar changes in thickness, stiffness, and contractility have been observed in aortic valve leaflets diagnosed with AVD; therefore, it is particularly important to study the biomechanics of hypertension with respect to the aortic valve. [4,5,41,61,68-73]

Aortic Valve Disease

Irregularities of the aortic valve can lead to aortic valve diseases, such as valve stenosis and/or regurgitation. To effectively manage aortic valve disease, traditional treatment algorithms should be followed: early gross diagnosis, noninvasive imaging, catheterization or angiography, and medical treatment until symptoms progress and indicate surgery is necessary. [4] Left untreated, aortic valve disease can result in heart failure, infection, and sudden death.

Aortic Stenosis

The term aortic stenosis refers to the narrowing of the aortic valve opening during systole. Two general types of aortic stenosis exist. The first is a congenital abnormality of the valve and is often detected in childhood. The second is caused by progressive calcium and scar tissue buildup. Scar tissue and calcium can collect on an abnormal congenital valve from damage due to rheumatic fever, or on the aortic valve leaflets gradually with age. The incidence of major aortic stenosis causes the left ventricle muscle to thicken in order to overcome the stress of the obstruction. The resulting thick muscle becomes stiff and causes a high pressure in the left ventricle when it fills with blood. This pressure is consequently transmitted to the lungs and generally causes shortness of breath in patients, and may potentially cause additional damage to the aortic valve. Other symptoms that accompany severe aortic stenosis include angina, dizziness, and possible sudden death. [74]

Aortic Regurgitation

The term aortic regurgitation refers to leakage in the aortic valve allowing a backwards flow of blood into the left ventricle during diastole. This form of valve disease can be caused by structural abnormalities of the valve. Enlargement of the aorta stretches the valve leaflets and produces aortic regurgitation. Acute onset of aortic regurgitation can occur as a result of either an infection of the aortic valve or a tear in the aorta. Chronic aortic regurgitation is often present for some time before any symptoms arise. The regurgitation

causes a large volume of blood to flow backward into the left ventricle. The ventricle compensates for the increase in blood volume by enlarging the cavity and increasing the thickness of the cardiac muscle. [74] Left ventricular compensation allows the heart to pump typical blood volume required by the body, plus additional blood that flows backwards into the ventricle. Symptoms that accompany severe aortic regurgitation are shortness of breath and chest pain. Long-term untreated aortic regurgitation results in irreversible damage to the muscle tissue of the left ventricle; in these cases an aortic valve replacement is necessary. [75]

Current Treatment Options

Often times, valvular pathologies slowly progress, making them difficult to diagnosis until surgical intervention is necessary. Over 100,000 valve replacement surgeries are performed each year. [2] Currently, several different treatment options, including bioprosthetic and mechanical aortic valves, are used to replace damaged or diseased aortic valves. Each replacement option has advantages and drawbacks; therefore, surgeons must choose the appropriate valve replacement to suit the patient's physiological needs and lifestyle.

Bioprosthetic Aortic Valves

Several different types of bioprosthetic aortic valves exist, including allograft and xenograft prosthesis, as shown in **Figure 7**. The major drawback of bioprosthetic aortic valve replacements is their tendency to wear out over time.

In older, less active adults, the bioprosthetic valve can operate effectively for 20 years or more; however, younger, active patients would require a secondary valve replacement surgery after approximately 10 years, due to deterioration of the valve and growth of the patient. [76-82] Nonviable allograft aortic valves are obtained from cadavers at autopsy, sterilized by incubation with low-dose antibiotics, and can be stored at 4˚C for weeks. Since the replacements are nonviable, they are unable to repair and remodel the valvular tissue in response to injury or high mechanical stress; therefore, they wear out quickly. Alternatively, viable allograft valves are collected from transplant donors and are cryopreserved within two hours of collection. Cryopreserved allograft valves are replaced less frequently than refrigerated valves because cellular activity slows deterioration. [83,84] Allograft valves are preferred over xenograft valves because they are structurally identical to the valve to be replaced; however, the supply is very limited. Porcine xenograft aortic valve replacements are similar in structure and hemodynamics to human aortic valves and are readily available, making them an ideal substitute for allograft valves. However, porcine valves must be fixed with glutaraldehyde for non-immunogenic purposes, a process that can lead to calcification. Also, xenograft aortic valves, similar to allograft valves, lack cellular activity and tend to degenerate due to mechanical wear. [85-87]

A  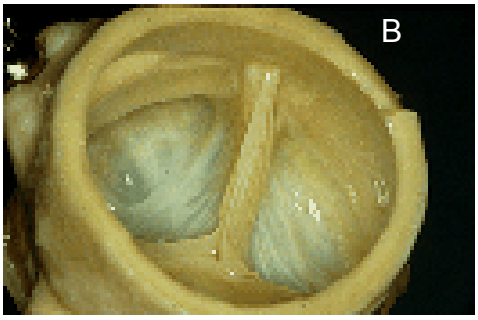

Figure 7: (A) Allograft (B) Porcine xenograft bioprosthetic valve (chelationtherapyonline.com)

Mechanical Aortic Valves

Mechanical valves are sometimes used as an alternative to bioprosthetic valves due to their durability; however, high shear stress across the implant activates platelets, causing thrombosis formation. [88] As a result, the patient would require lifelong anticoagulation therapy. Ideally, mechanical valves would prevent regurgitation while minimizing shear stress and turbulent blood flow. [89-91] Similar to bioprosthetic valves, mechanical valves are best suited for mature adults, and patients typically require replacement surgery after approximately 20 years. [76,77,79,88,89] Several different types of mechanical valve replacements exist, including caged ball, tilting disk, and bileaflet valves, all shown in **Figure 8**. [88,92] Caged ball valves oscillate a rubber ball within a cobalt-chromium alloy cage to regulate blood flow between the left ventricle and the aorta via changes in pressure gradients. The drawback to using caged ball valves is that they produce a higher amount of turbulent flow compared to replacement valves that

utilize rotating disks. [93] Tilting disk valves use a single, circular disk held by wire-like arms, whereas bileaflet valves employ two semicircular leaflets connected by hinges. Typically, these disks are made of stainless steel, titanium, silicone, or pyrolytic carbon and are sewn into the patient via double velour, knitted polyester cuff. [94] Having been implanted into around 600,000 patients, bileaflet valves are the most popular mechanical valve as compared to the tilting disk valve and ball-and-cage valve, having 360,000 and 200,000 implantations, respectively. [93]

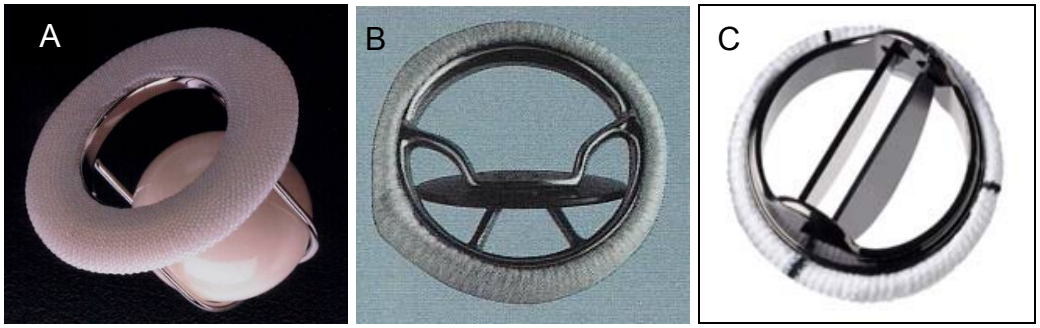

Figure 8: Mechanical valves (A) Starr-Edwards caged ball (baxter.com) (B) Sorin Medical tilting disk (sorin.com) (C) St. Jude's bileaflet (sjm.com)

Tissue Engineered Aortic Valves

Due to the limitations of bioprosthetic and mechanical valves, engineers are currently striving to tissue engineer a replacement aortic valve that is non-thrombogenic, able to withstand dynamic mechanical stress, and remodel and grow with the patient. To do so, engineers have attempted to create a viable tissue that is able to respond to the body's needs and develop along with the patient. [95] Recreation of aortic valve tissue function requires researchers to first

understand the aortic valve response to stimuli. Study of aortic valve biology and mechanics have lead to the development of two fundamental strategies, including biodegradable polymeric scaffolds, and non-degrading biological matrix scaffolds.

Biodegradable polymers repopulated with autologous cell types are the most widely used strategy. Both separately and in combination, poly(lactic-*co*-glycolide) (PGLA), poly-3-hydroxyoctanoate (PHO), and polyhydroxyalkanoate (PHA) have been used as biodegradable polymers in valve design due to their mechanical properties, melting temperatures, biocompatibility, and degradation time. [96] After implantation, the polymer begins to slowly degrade and the active cell types within the polymer generate biological matrix to compensate for polymer degradation. Essentially, new, viable valve tissue is created in the absence of the polymer scaffold; however, this strategy has failed to produce satisfying results. Polymer degradation via hydrolysis alters pH of the valve's biochemical environment, leading to undesired cell death and differentiation, offering a possible explanation of failure. [97,98] An additional source of malfunction may be due to the use of vascular autologous cells rather than valvular cells, which have shown to have different phenotypes and mechanical behavior. [25]

The alternative strategy, biological matrix scaffold valve replacement, is less developed than the previously discussed valve design. Collagen, fibrin, and chitosan have been used as possible valve matrix materials, both in combination and independently. [99-101] The advantages of using solely biological material for

valvular scaffolds is the wide availability of these materials from xenogenic sources, the ability to accommodate cellular growth, ease of processing, and lack of cytotoxic degradation by-products. Although advantageous, the use of biological matrix scaffolds has yet to produce a material capable of withstanding native valve's harsh, dynamic, mechanical environment. [102] Bioprosthetic and mechanical valves will continue to be used as valve replacements; however, scientists refuse to surrender to this challenge and will continue to explore different bioengineering alternatives and techniques until a suitable tissue engineered valve replacement is created. In the meantime, further research is necessary to fully understand the origin and progression of aortic valve disease. The ultimate goal is to avoid valve replacement surgery by early intervention and the development of non-invasive therapy, thus improving the patient's quality of life.

Objective of the Study

The objective of this study was to investigate a change in α/β-myosin heavy chain expression, if any, of aortic heart valve leaflets due to varying magnitudes of transvalvular pressure. In order to achieve this objective, two goals must be accomplished: (1) a cyclic transvalvular pressure bioreactor must be created, and (2) myosin expression must be evaluated after exposing aortic valve leaflets to varying levels of pressure.

Scope and Limitations of the Study

This study concentrates on the response of aortic valve leaflets exposed exclusively to cyclic transvalvular pressure, independent of other mechanical and biochemical stimuli. Rather than studying how the valve responds to multiple forces simultaneously, the bioreactor allows researchers to focus on the direct effects of pressure to valve mechanobiology. As previously stated, aortic valve disease is associated with high transvalvular pressure and diastolic strain across the aortic valve leaflet; therefore, the bioreactor will only be required to cycle between, at least, 60mmHg and 80mmHg, for physiological conditions, and 60mmHg to 100mmHg for pathological conditions. Systolic transvalvular pressure has little to no effect on leaflet strain. [58] Also, Shin et al. demonstrated that pressure magnitudes between 20-60mmHg did not cause significant changes in endothelial barrier function; therefore, systolic transvalvular pressure will be neglected. [103] Preliminary studies of aortic valve mechanobiology as a result of transvalvular pressure will focus on changes in cellular phenotype with respect to α/β-myosin heavy chain. Healthy valves are passive by nature, opening and closing as a result of pressure gradients rather than muscle contraction; however, this study will elucidate the cellular response of myofibroblast differentiation from fibroblasts to smooth muscle cells observed during valve remodeling and disease. [9,34,40]

CHAPTER II

DESIGN OF A CYCLIC PRESSURE BIOREACTOR

Brief History of Heart Valve Bioreactors

To investigate cellular and tissue responses to mechanical stimuli, bioreactors are used to simulate the valve's biomechanical and biochemical environments. [104-107] *Ex vivo* and *in vitro* experimental models provide a cost effective alternative to *in vivo* animal models, due to the high costs of purchasing, housing, feeding, and providing care for the animals used in testing. Bioreactors are typically used for regulatory clearance tests on prospective valve replacement options prior to FDA approval. [108] They are also used for mechanically conditioning tissue engineered valve constructs due to the mechanosensitivity of valvular cells. [104] However, the long term goal of valvular study within a bioreactor is to predict tissue structure and function by studying cell, scaffold, media, and environmental conditions, thus providing a rational basis for future tissue engineering design. [108] Previously, bioreactors have been constructed to study the valvular response to both tension and shear stress. [109,110] Flexural stress has also been simulated in a laboratory setting; however, the majority of bioreactors mimic the pulsatile blood flow across the valve leaflet, thereby testing the valvular response to both pressure and shear stress. [107,111-115]

Xing et al. created a bioreactor to study the effects of cyclic pressure with no other mechanical interference; however, Xing cycled pressure between 80mmHg and 120mmHg, rather than studying transvalvular pressure correlated to mechanical stress. Also, Xing compared the aortic valve's biological response between pressure levels of 80-120mmHg, 120-160mmHg, and 150-190mmHg, all of which had a 40mmHg difference in pressure. [116] To elucidate the effects of transvalvular pressure with increasing amplitudes, a cyclic pressure bioreactor will be created.

Design Requirements

To create a bioreactor that adequately mimics the dynamic transvalvular pressure levels across the aortic valve, the system must cycle between at least 60 - 80mmHg for normotensive conditions, 60 - 90mmHg for Stage I hypertension, and 60 - 100mmHg for Stage II hypertension. The bioreactor should cycle at a frequency of 1Hz, which correlates with a heart rate of 60 bpm. At this frequency, the pressure should gradually increase to the target pressure for approximately 0.6 seconds to simulate the aortic valve being closed during diastole; the pressure should then drop to atmospheric pressure for 0.4 seconds to simulate the aortic valve being open in systole with no pressure across the leaflet, and repeat. The culture media contains additives and growth factors to supply nutrients to the samples. To ensure proper gas exchange and maintain ideal pH levels in the media, the bioreactor must sustain 100% humidity with 5% CO_2. [117] Also, the bioreactor must be able to fit within a standard incubator at

37˚C to keep samples at normal core body temperature. Finally, the bioreactor must be able to be sterilized to prevent tissue contamination and have a user friendly interface for consistent and accurate operation.

System Overview

The system consisted of a chamber in which to place samples and produce cyclic pressure, solenoid valves (McMaster-Carr, 4868K11) to control the timing of the pressure cycle, and a computer to control electrical devices. The pressure was monitored using a pressure transducer (Omega Engineering, Inc., PX302-200GV) connected to the front of the chamber, and the signal was conditioned using a load cell conditioner (Encore Electronics, Inc., Model 4025-101). To produce a 5% CO_2 environment within the chamber and control the amount of pressure added to the system, the air supply solenoid valve was connected to a ten gallon air tank containing 5% CO_2 and a pressure regulator. Also, to prevent backflow of pressure, the air supply valve was connected to a bronze spring-loaded ball check valve (McMaster-Carr, 47715K41). The computer controlled the electrical devices via a data acquisition (DAQ) module (Measurement Devices, PMD1608) and custom written software (LABView, National Instruments).

Materials

Pressure Chamber Materials

A scratch resistant acrylic cylinder (McMaster-Carr, 8486K937) was used to build the chamber of the bioreactor, which allowed the researcher to observe the samples during testing. The cylinder had an outer diameter (OD) of 6", an inner diameter (ID) of 5.5", and was 10" in length. The aluminum end plates were 1" thick and had a 0.5" pilot with a 5.5" diameter that fitted tightly inside the acrylic cylinder. The front end plate had a ¼" national pipe thread (NPT) hole through the center of the plate, so the pressure transducer could read the pressure from inside the chamber and send the information to the computer via the DAQ module. The rear end plate had two ¼" NPT holes, one through the center of the plate for the exhaust solenoid valve, and the other 2" above center for the air supply solenoid valve. The rubber diaphragm within the solenoid valve blocked the flow of air until electrically stimulated, as illustrated in **Figure 9**. Only a 1 psi pressure differential was required to raise the lightweight, viton diaphragm, which made the valve more energy efficient than most valves. Diaphragm pilot-operated solenoid valves have a higher flow rate than both direct-acting and piston pilot-operated valves, which made them an ideal choice for rapid pressure influx and exhaust.

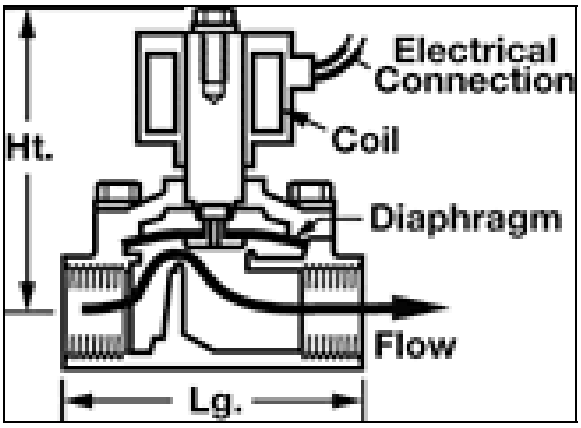

Figure 9: Schematic of operation of normally-closed viton diaphragm solenoid valve

(mcmaster.com)

A ten gallon air tank with 5% CO_2 was connected to the air supply solenoid valve via pressure regulator to create a pressurized environment suitable for tissue culture. To prevent loss of pressure, the pilot of the rear end plate had a 0.125" grove fitted with a 70 Duro o-ring (Hercules, 252) with a 5.5" OD and a 5.25" ID to create a tight seal between the pilot and the acrylic cylinder, thus making the plate difficult to remove. Nitrile was placed around the pilot on the front plate, so it could be easily added and removed between experiments without disrupting the samples. The two end plates were held together by four threaded rods in each corner, tightened with nuts. The SolidWorks drawings of the pressure chamber used in the system can be seen in **APPENDIX A**, whereas actual pictures of the bioreactor are found in **APPENDIX B**. A ¼" thick aluminum plate was used within the chamber to provide a flat surface within the cylinder on which to rest the samples. The plate was 4.5" x 8" and had an area large enough

to support up to four 4" x 6" sample plates used in testing. A water reservoir was also placed on top of the sample plate to create a 100% humidity environment within the system. A dissected side view of the pressure chamber, which illustrates where the sample plate is located within the cylinder, can also be found in **APPENDIX A**. Total volume of the chamber used to hold pressure, excluding the volume of the pilots and sample plate, was 846.8 in^3.

Electrical Devices Used

The pressure transducer was connected to the Analog In port 0 of the DAQ module via BNC coaxial cables (RG-58, 50Ω) so LabVIEW could create a continuous pressure versus time graph during testing and record the pressure. A graph of the signaling of the air supply solenoid valve was produced by connecting a wire from the air supply valve to the Analog In port 1, thus ensuring the experimenter that the valves were signaled properly. A 220Ω resistor, transistor, and relay were connected in series, respectively, and were used to control the activation of the solenoid valves. The air supply and exhaust solenoid valves were connected to the DAQ module in Digital Out ports 0 and 1, respectively. While the valve was uncharged, there was no current across the resistor and the transistor was automatically grounded. However, when the computer sent a signal across the resistor to turn on the valve, immediately thereafter the transistor connected the circuit, and the signal ran through the relay. A three-pronged electrical extension cord was used to power the relay, and was connected to the solenoid valves and relays as shown in **APPENDIX C**.

The computer sent a 5V signal to turn on the relay via DC current and activated the valve to remain open for the specified amount of time. A complete schematic drawing of the electrical devices is shown in **APPENDIX C.**

Procedure Used to Run Bioreactor

Prior to experimentation, the bioreactor was sterilized with a 70% ethanol solution. The LabVIEW user interface had a switch marked "TEST" which allowed the user to test each valve prior to experimentation to ensure proper function and signaling from the computer. The LabVIEW interface prompted the user to provide the amount of time the system cycled in diastole and systole, 0.6s and 0.4s respectively, which controlled the timing of the valves when switched to "RUN". LabVIEW used this information to properly signal the air supplier and exhaust solenoid valves. The program could allow researchers to not only test normal physiological heart rate, but also varying pathological heart rates. The user was also prompted to choose a sampling rate, which told the computer how many pressure and signal readings to record per second. The maximum sampling rate of the pressure transducer used for the bioreactor was 10 samples per second. Also, the computer asked the user for a Microsoft Excel file in which to store the time, pressure, and signal readings, so the researcher was able to review the pressure readings and ensure there was no drop in pressure or improper signaling during testing. LabVIEW then created a signal and pressure versus time graph, a waveform showing when the air supply valve was turned on

and off, as well as a saw tooth waveform mimicking transvalvular pressure during the cardiac cycle.

Sterility Tests

Prior to experimentation, the bioreactor was sterilized using a 70% ethanol solution. Using sterile technique, the samples were placed inside the chamber, which was then sealed to create an air-tight environment for testing. The pH and absorbance of the medium involved in this study was compared prior to and after 11 hr of experimentation using a pH meter and spectrophotometer at 365nm, respectively. A significant increase in medium pH or absorbance was considered to imply the bioreactor had microbial growth or contamination, hence regarded as a non-sterile environment for testing.

Results

The sterility tests measured by medium pH and absorbance indicated no significant change occurred after 11hr of culture. The pH of the medium prior to and after experimentation was 7.4, indicating no change in medium pH. The media absorbance prior to testing was 0.5304±0.0099, whereas the absorbance following testing was 0.5652±0.0296 ($p>0.05$; paired t-test), indicating no microbial contamination; therefore, cleaning the sample surface of the bioreactor with a 70% ethanol solution was suitable for container sterilization. In addition, the ten gallon air tank containing 5% CO_2 balanced with air allowed for 10.7 ± 0.205 hr of experimentation. Also noted, the temperature of the media after an

hour of experimentation dropped from 37˚C to 34.7˚C. The pressure chamber met all of the system requirements of a cyclic pressure bioreactor for aortic valve study. The chamber (1) fit into a standard humidified incubator at 37˚C, (2) perfused air with 5% CO_2 to maintain pH and efficient gas exchange, (3) maintained sterility throughout testing, and (4) cycled between diastolic transvalvular pressure levels for physiological and pathological conditions. **Figure 10** shows the simulation of the pressure levels used during valvular testing.

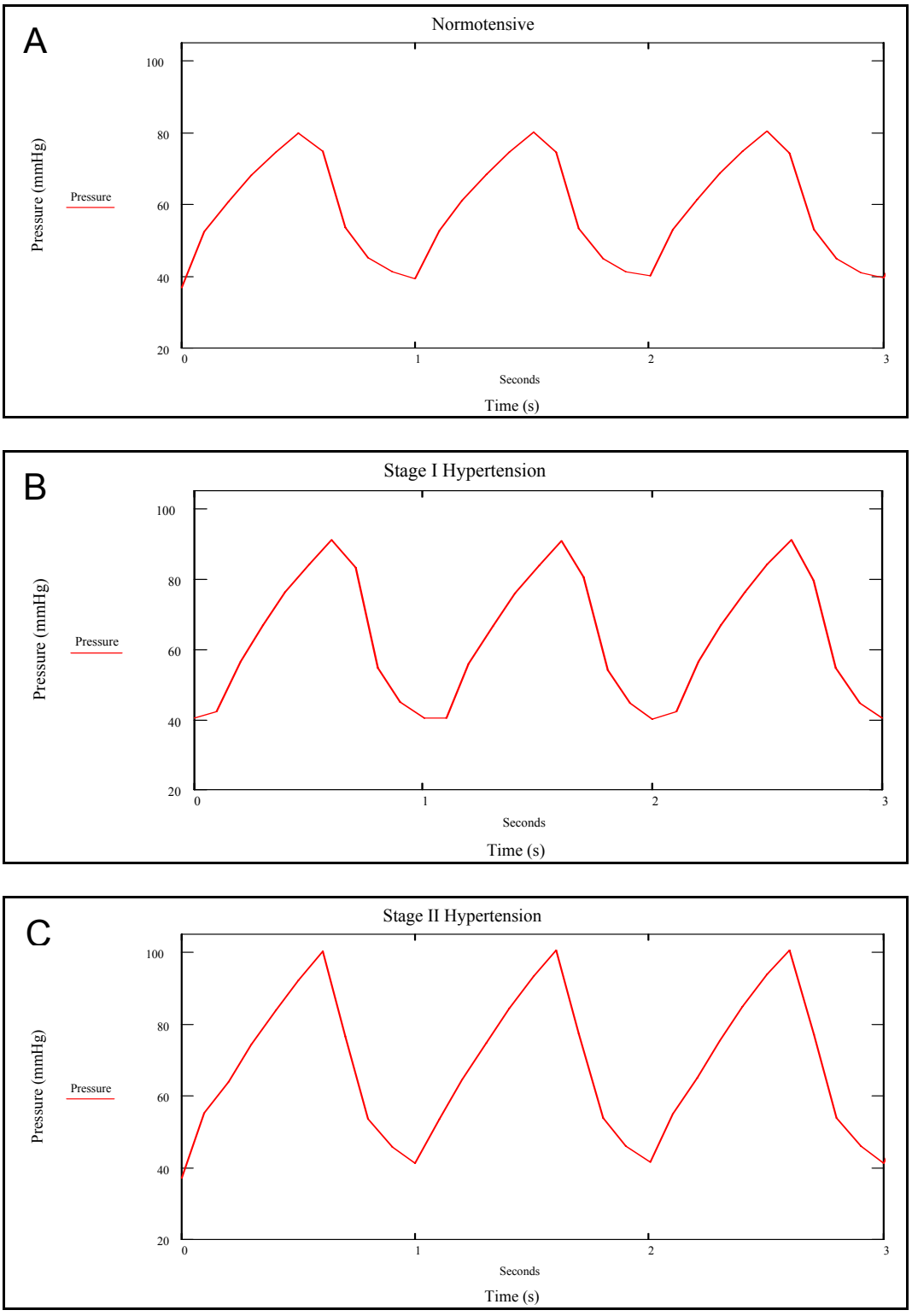

Figure 10: Graph of pressure simulation within bioreactor at (A) normotensive, (B) Stage I hypertensive, and (C) Stage II hypertensive conditions

Discussion

The bioreactor created for this study met all of the functional requirements and was successful in overcoming the limitations of the bioreactor previously used within this research group. The previous pressure system consisted of a stainless steel chamber with a 6.5" OD and 6" ID, and used a pneumatic cylinder controlled by a waveform generator. Since the bioreactor was made of stainless steel, it was extremely heavy, difficult to maneuver, and lacked transparency, which prevented sample observation during testing. In contrast, the current design was made of an acrylic cylinder and aluminum plates, which were of moderate weight, easily maneuvered, and transparent. The area allotted for testing in the previous bioreactor only allowed for two sample plates to be tested simultaneously, whereas the current model easily accommodated four sample plates at one time. Regarding functional requirements, the previous design was limited by the magnitude and frequency of the waveform generated, due to the incompressibility of air and lack of utilization of an exhaust valve. Without a valve to allow a quick exhaust of pressure, the air used to produce the pressure had no escape besides what was removed on the backstroke of the cylinder. For this reason, higher pressure levels that required more air be added to the system, in turn required more time to allow the pressure to drop, thus reducing the frequency. The current design, however, utilized an exhaust valve and was therefore able to reach desired pressure magnitudes without affecting the

frequency of the waveform. Overall, the current design is superior to the alternative in performance and convenience.

The bioreactor successfully exposed aortic valve leaflets to cyclic transvalvular pressure with respect to diastole of the cardiac cycle; however, the experiment was limited by the amount of time each experiment can be run. Cellular differentiation into different phenotypes as a result of mechanical stress may require more than ten hours of exposure to cyclic pressure; therefore, it is important for the bioreactor to be capable of testing for extended periods of time. To overcome this limitation, multiple air tanks can be connected to the bioreactor for extended use, or possibly, an air return system can be created to constantly cycle the exhaust air back into the chamber for continuous use. The latter option may result in a loss of CO_2 due to tissue gas exchange; therefore, experimenters should be aware of this issue.

Also, it was important to note that the 2.3°C drop in media temperature was possibly due to the rapid influx of air mixture from a room temperature air tank. The decreased media temperature may have little to no biological side effects; however, to overcome this potential limitation a small heater can be used to maintain media temperature by warming the aluminum sample plate on which the samples rest. This design alteration will require further investigation to prevent overheating the media and should also utilize a temperature regulator to maintain a consistent sample plate temperature, and as a result, media temperature.

Aortic valve disease has only been associated with high diastolic pressure; however, if both systolic and diastolic transvalvular pressure are to be simulated (requiring the pressure to drop to zero rather than 40mmHg), a vacuum pump and reservoir could possibly be connected to the exhaust solenoid valve. The vacuum pump could be set to remove a fixed amount of pressure so when the exhaust valve opens, the amount of air required to completely drop the pressure from the set pressure level would be drawn into the vacuum reservoir. The removal of the pressure would create a 0mmHg environment synonymous with systolic transvalvular pressure. Conversely, when the exhaust valve closes, the vacuum will no longer affect the chamber and will allow the pressure to increase via pressurized air. This design, however, has not been tested and will require further investigation.

In addition to testing aortic valves at varying pressures, it may be prudent to study the effects of varying frequencies as well. For example, the effects of changes in heart rate before, during, and after surgery could elucidate changes in protein expression within the valve, and possibly explain why postoperative arrhythmias occur in up to 20% of patients. [118-121] The LabVIEW program used for this bioreactor allows the experimenter to choose the length of time air enters and leaves the chamber; therefore, the frequency of the cycle can easily be adjusted. The bioreactor allows for a maximum frequency of 1.5Hz (90bpm) due to the amount of time required to exhaust the pressure from the system. As seen in the results, a major pressure decrease occurred in the first 0.2s after exhaust

valve activation, then gradually declined to the residual pressure for the remaining 0.2s of exhaust. The average pressure drop in the initial 0.2s of exhaust was 45.8 ± 0.34mmHg, measured over 20 pressure cycles. Given that testing Stage II hypertensive conditions only requires cycling pressure between at least 60-100mmHg, a frequency of 1.5Hz allows 0.22s for exhaust, which is ample time to drop 40mmHg of pressure. If a vacuum pump is attached to the exhaust valve, it could facilitate a faster drop in pressure and would allow higher frequency testing. The minimum frequency of the bioreactor is not limited, however, because the pressure regulator could allow slow influx of air and the exhaust valve would have sufficient time to drop the pressure within the reactor.

To completely reduce the pressure from 100mmHg to 0mmHg requires 1.20±0.04s, reported from data analysis of 20 pressure cycles. Since the amount of time the aortic valve is closed is approximately 2/3 of the cardiac cycle, the influx of air into the pressure chamber would require 2.4s to create the same balance of valve opening and closing experienced in physiological conditions. As a result, a frequency of 0.28Hz would be used for testing the effects of both systolic and diastolic transvalvular pressure levels on aortic valve mechanobiology. Besides using a vacuum pump to increase the frequency and closer mimic physiological conditions, an exhaust valve with a larger diameter can be used to drop the pressure within the bioreactor more quickly. Currently, the 3/8" diameter exhaust solenoid valve has a flow rate of 3.3 gallons per minute (at 60°F, specific gravity of 1); whereas, an exhaust valve with a 2" diameter has

a flow rate of 28.0 gallons per minute. A larger diameter solenoid valve is more cost effective than using a vacuum pump to increase bioreactor frequency, however may not be able to drop the pressure completely to zero within physiological range and should therefore be investigated further.

In conclusion, a sterile culture system has been constructed to allow study of porcine aortic heart valve mechanobiology *ex vivo*. The pressure within the bioreactor cycled between diastolic transvalvular pressure levels for physiological and pathological conditions. To meet system requirements, the bioreactor was compact and could therefore be contained within a humidified incubator to maintain tissue temperature at 37˚C. An air tank containing 5% CO_2 allowed gas exchange to sustain a pH of 7.4 within the culture medium. Furthermore, the pressure magnitude and frequency were controlled independently, allowing a wide range of conditions to be studied.

CHAPTER III

PRELIMINARY STUDY OF α/β-MYOSIN EXPRESSION

Introduction

Myosin heavy chain isoforms have been used to study smooth muscle cell differentiation, as well as the cellular mechanisms of atherosclerosis. [122] Since aortic valve disease is associated with atherosclerosis and interstitial cell differentiation into smooth muscle cells, it is prudent to study the expression of myosin within the aortic valve. As previously stated, three forms of myosin heavy chain exist: (1) α-MHC, (2) α/β-MHC, and (3) β-MHC. Alpha- forms are characterized as fast-twitch muscle fibers, whereas beta- forms are classified as slow-twitch muscle fibers. The α/β-MHC show characteristics of both α- and β-MHC, and are therefore considered the transdifferentiated form of myosin. Interstitial cells that have differentiated into smooth muscle cells in response to mechanical stimulation or injury express both α- and α/β- myosin heavy chain; however, myosin within valvular endothelial cells has yet to be classified and requires further investigation. [9] Previous studies have shown that hemodynamic stimuli affect MHC gene expression; therefore, increased cyclic pressure may cause amplification of myosin expression indicating a higher degree of fibroblast differentiation, thus valvular remodeling. This study will examine the effects of

cyclic transvalvular pressure on cellular differentiation via α/β-myosin heavy chain expression in porcine aortic heart valve leaflets. [123]

Methods

Aortic valve leaflets were extracted from adult pigs within 10 min of slaughter at a local abattoir (Sansing Meat Service, Maben, MS, USA). Five aortic valve leaflets were fixed in 10% formalin (Fisher Scientific) immediately following excision to serve as a control group. Leaflets used in testing were placed in Dulbecco's phosphate-buffered saline (PBS; Sigma) and transported to the laboratory. Upon arrival, the leaflets were placed in 6-well plates with 5mL of Dulbecco's Modified Eagle Medium (DMEM; Sigma) supplemented with 1% Anti-biotic/Anti-mycotic solution (ABAM; Sigma) and 10% fetal bovine serum (FBS; Mediatech Inc.). Samples were then placed in a humidified incubator for 24 hours with 5% CO_2 to allow the leaflets to adapt to the culture media before experimentation. The protocol for leaflet extraction and culture can be found in **APPENDIX E**. Five leaflet samples were fixed after 24 hours of incubation to serve as secondary controls. Two hours prior to cyclic pressure experimentation, the bioreactor was placed within the humidified incubator to allow temperature stabilization within the testing chamber. Five leaflets were place inside the bioreactor and programmed to cycle from 40 – 80mmHg, simulating normotensive transvalvular pressure. The same process was repeated at 40 – 90mmHg to test Stage I hypertensive conditions, and 40 – 100mmHg for Stage II hypertensive conditions. Each experimental run was tested under cyclic

conditions for approximately 10hr, after which the samples were placed in a 10% formalin fixative solution. After fixation, the samples were embedded in paraffin and immunohistochemistry was performed to investigate changes in the cell phenotype due to increasing cyclic pressure with regards to α/β-MHC (GeneTex, Inc., GTX20015). The protocol used for antibody staining can also be found in **APPENDIX E**. Heat-induced epitope retrieval was used to produce markedly, improved antigen staining and also helped overcome false negative staining of over-fixed tissue. Prior to heat exposure, the slides were submerged in a 10x Target Retrieval solution (DAKO Corp., 51699) diluted to a 1:9 ratio using distilled water. The slides were then placed inside a steamer for 30 minutes for previously described epitope retrieval, then rinsed in distilled water and placed in TRIS Buffer Saline (DAKO Corp., 5196830) until immunohistochemistry was to be performed. The primary antibody, α/β-MHC, was optimized to a 1:800 dilution and utilized antibody diluent (DAKO Corp., 5080983). Secondary antibodies, biotinylated link (yellow) and streptaradin horse reddish peroxidase (red) (LSAB2 System, DAKO Corp., K067589) were used to bind to the primary antibody and increase the expression of the stain. In addition, diaminobenzidine tetrahydrochloride (DAB) (DAKO Corp., K346689) was used to form a brown stain indicating positive expression of the α/β-MHC antigen in the end-product. Furthermore, hydrogen peroxidase was used to block tissue endogenous peroxidase activity and IgGI mouse (DAKO Corp., X0931) was used for a negative control. The final step in the immunohistochemistry procedure involved

counterstaining the slides. Hematoxylin solution (Sigma-Aldrich, GHS332-1L) was used to stain the nucleus of the cells blue and a 0.3% ammonia water solution (1.5mL of ammonium hydroxide with 500mL of distilled water) tinted the slides a bluish color.

Results

The results showed a random distribution of interstitial cells throughout the leaflet, and a positively stained endothelium that slowly detached and lost protein expression over time. **Figure 11** shows an aortic valve leaflet fixed immediately after excision with an intact arterial endothelium stained heavily for α/β-MHC. The same leaflets also stained positive for myosin sporadically within the subendothelial layer, as shown in **Figure 12**. After 24 hours of culture, the endothelial layer began to detach, however continued to stain positive for α/β-MHC, as did a few smooth muscle cells in close proximity to the endothelium, seen in **Figure 13**. The five leaflets placed in the pressure chamber at normotensive and Stage I hypertensive conditions showed no myosin staining except occasionally at the site of extraction, displayed in **Figure 14** and **Figure 15**. Leaflets exposed to Stage II hypertensive pressure levels showed no α/β-MHC staining except for one area located on the fibrosal endothelium, seen in **Figure 16**.

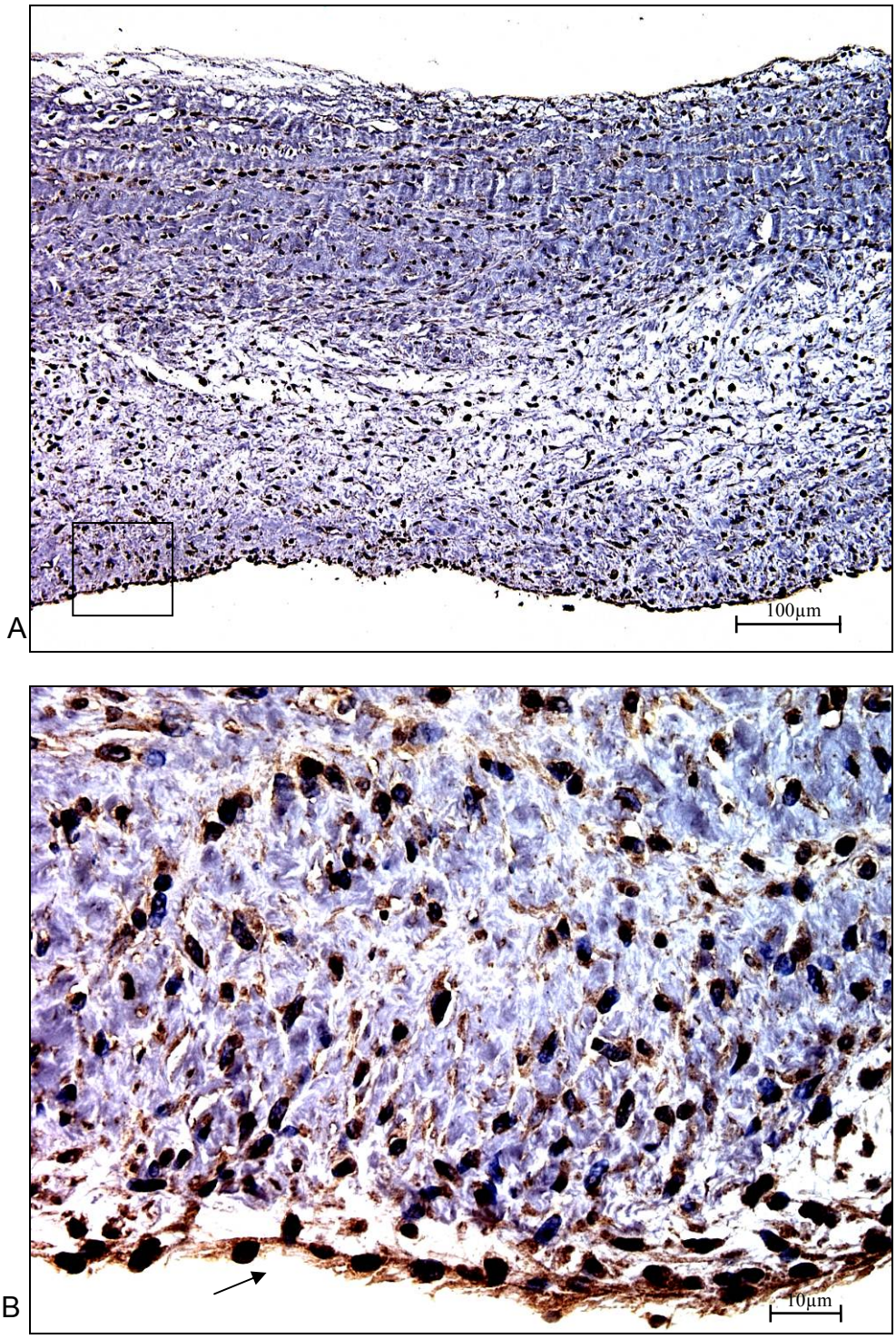

Figure 11: Immunohistochemistry of α/β-myosin heavy chain of leaflet fixed immediately after excision (A) 10x (B) 40x (focused on endothelium).

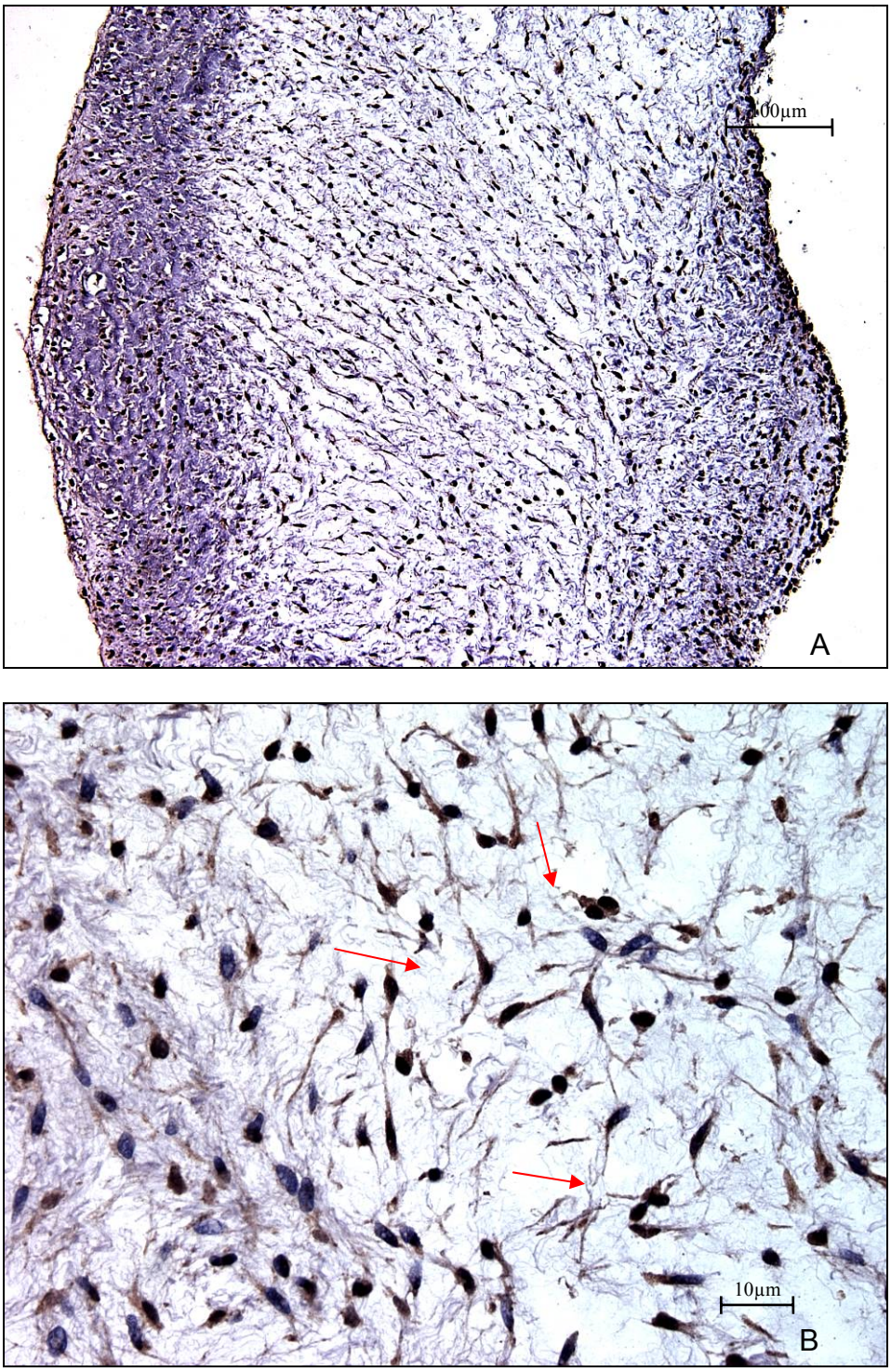

Figure 12: Immunohistochemistry of α/β-myosin heavy chain of leaflet fixed immediately after excision (A) 10x (B) 40x (focused on spongiosa layer).

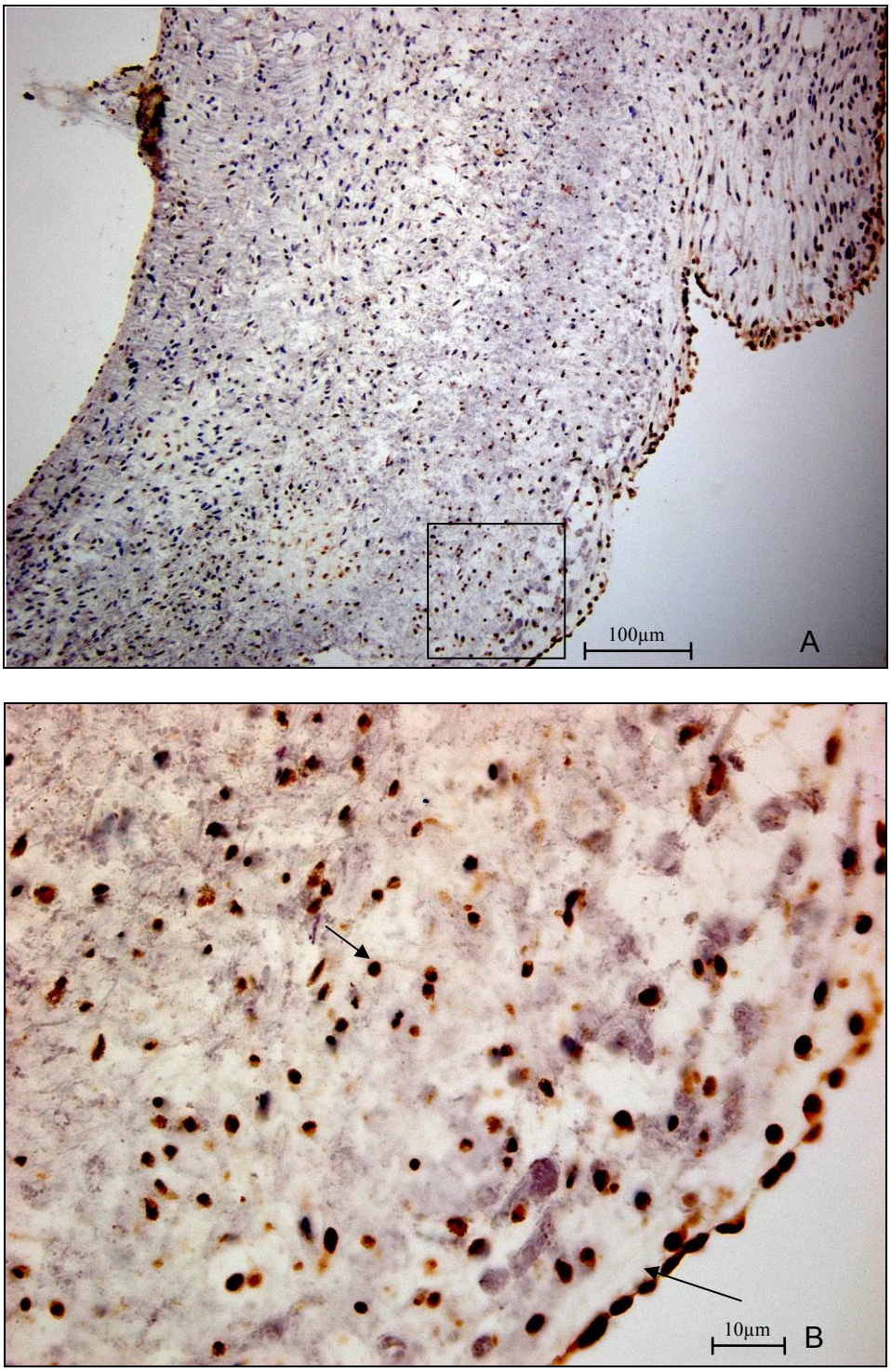

Figure 13: Immunohistochemistry of α/β-Myosin heavy chain after 24 hours in media (A) 10x (B) 40x (focused on fibrosal endothelium and spongiosa)

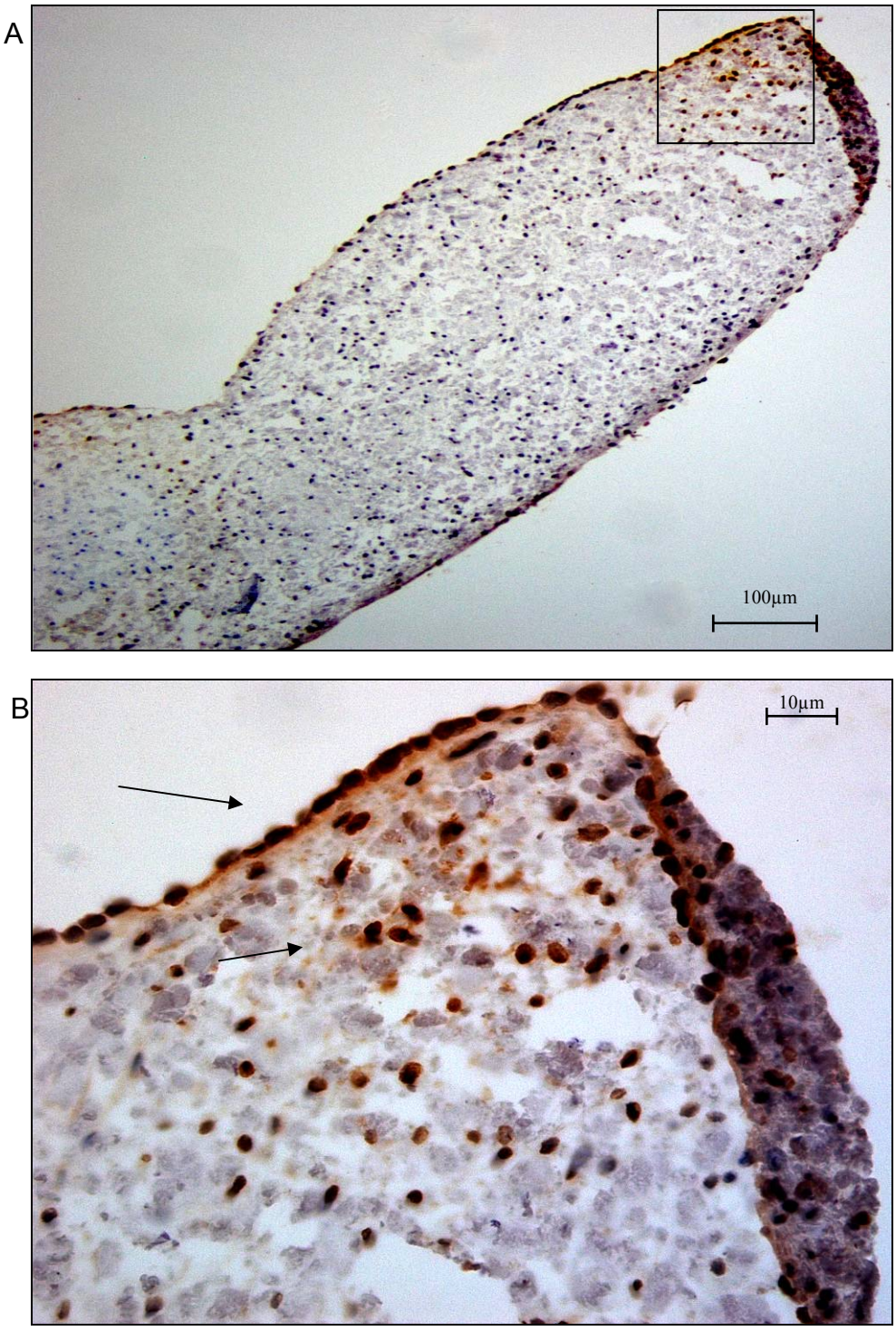

Figure 14: Immunohistochemistry of α/β-Myosin heavy chain exposed to 40-80mmHg cyclic pressure (A) 10x (B) 40x (focused on site of excision).

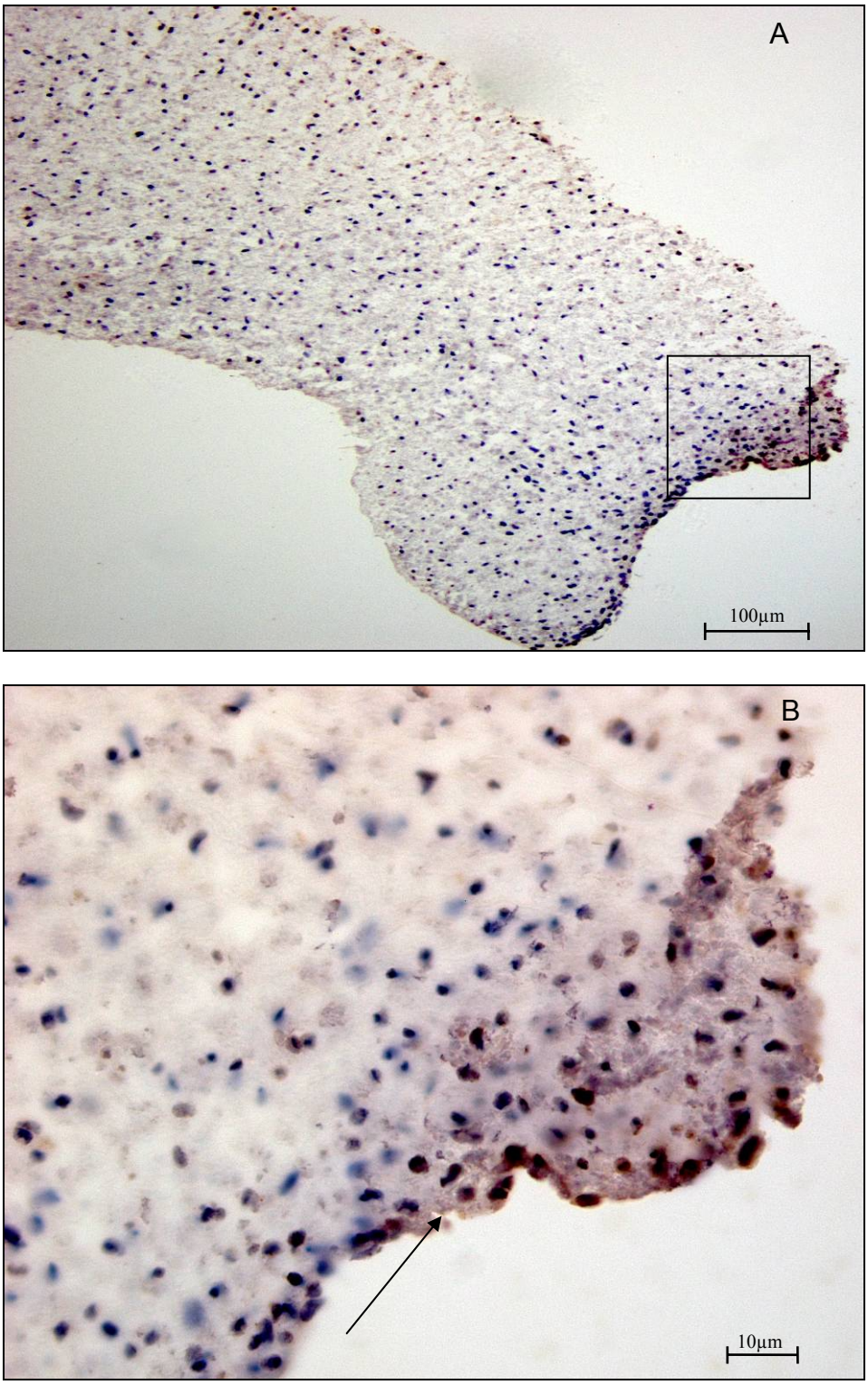

Figure 15: Immunohistochemistry of α/β-Myosin heavy chain exposed to 40-90mmHg cyclic pressure (A) 10x (B) 40x (focused on site of excision).

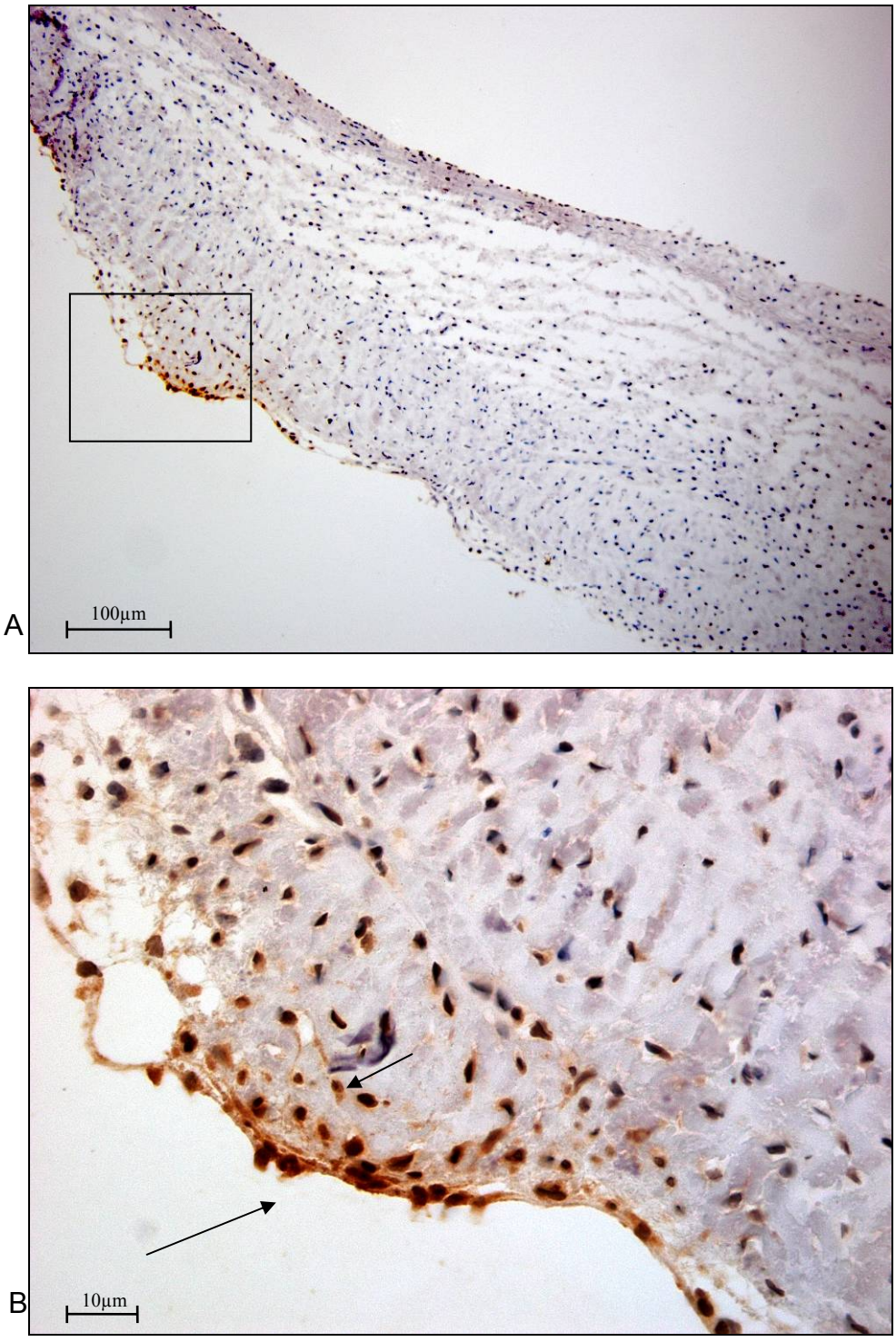

Figure 16: Immunohistochemistry of α/β-Myosin heavy chain exposed to 40-100mmHg cyclic pressure (A) 10x (B) 40x (focused on fibrosal endothelium).

Discussion

This study showed that α/β-myosin heavy chain is present in the arterial endothelial layer, and in smooth muscle cells within the subendothelial space of porcine aortic valves. As discussed earlier, the presence of smooth muscle cells indicates that the valve is undergoing remodeling. When the mechanosensitive endothelial layer recognizes an alteration in hemodynamics, it signals the interstitial cells to repair or remodel the extracellular matrix accordingly. The quiescent fibroblast population of interstitial cells differentiates into myofibroblasts, and if necessary, further differentiates into smooth muscle cells. The actual functions of the three phenotypes within the aortic valve are currently unknown but are under investigation.

After 24 hours of incubation the endothelial layer begins to detach, and myosin expression tends to decrease. Loss of the endothelial layer may be due to insufficient mechanical stimulation required for cellular function. Metzler et al. showed that 0-10% cyclic strain maintains the integrity of the valvular endothelial monolayer without inducing a pro-inflammatory response, indicating a strain range near that of physiological conditions; therefore, cyclic strain may be required to keep the endothelial layer intact. [124] Furthermore, normotensive and Stage I hypertensive conditions showed no myosin on the slowly denuding endothelium, except sporadically at the sites of extraction. One leaflet stimulated by Stage II hypertensive conditions stained positive for α/β-MHC on a single node of endothelial and subendothelial cells; however, no other myosin was found.

The node found on a Stage II hypertensive leaflet was discovered near a penetration site, possibly caused by tweezers during extraction. The subsequent damage to the endothelium and extracellular matrix was again possibly due to the high mechanical stress induced by the tweezers. The temporal limitations due to the single ten gallon gas tank setup, as previously described, may have contributed to the observed lack of cellular differentiation. Cellular response to mechanical stimuli is often characterized following up to 72 hours of exposure, to meet this time demand would require a multiple stage tank system or gas return mechanism.

Since the majority of α/β-MHC expression was found on the endothelial layer, this indicates the importance of keeping the endothelium intact. Additional studies of myosin heavy chain expression within the aortic valve may involve the creation of a biaxial cyclic strain device to maintain an intact endothelial layer. The biaxial strain device should be sterile, noncorrosive, and able to fit within the specifications of the pressure chamber. Also, additional programming would be required to synchronize cyclic strain with cyclic pressure at adjustable heart rates. If created, numerous studies could be performed involving variations of pressure, cyclic strain, and heart rate.

As mentioned earlier, the developing heart initially expresses only β-MHC and eventually converts completely to α-MHC when fully developed, with α/β-MHC as the transitional form. [47,49,50] When the mechanical environment in the heart becomes unstable, myosin reverts to its embryonic form, as shown by no α-

MHC expression at end-stage heart failure. [51] To date, the expression of myosin within the valve has been understudied. An interesting study would be to investigate what forms of myosin are expressed during valvulogenesis (assumedly β-MHC), and compare the expression of each of the three forms of MHC in mature leaflets exposed to physiological and pathological conditions. With this study, investigators could discover whether or not the valve reverts to its embryonic form as a result of changes in mechanical stimuli similar to the cardiomyocytes of the heart.

Possible evidence of valvular redifferentiation to the embryonic state is the deposition of calcium in diseased valves. During valvulogenesis, bone morphogenic protein (BMP) is among many molecules involved in epithelial mesenchymal transformation. [125,126] BMP-2 induces the expression of periostin, responsible for regulating collagen I fibrillogenesis and mediating matrix maturation. [19,22,127] The exact pathways involved in valvulogenesis pertaining to BMP and periostin expression are currently under investigation; however, alteration of the valve's mechanical and biochemical environment may reverse and disrupt these pathways, causing bone (rather than collagen) to form within the valve. Calcium deposits typically form at bending sites, synonymous with sites of initial embryonic cushion formation. Additionally, BMPs are known to be involved in the inflammatory response, which further implicates their role in valve calcification.

In conclusion, α/β-MHC was expressed in porcine aortic valve leaflets; however, due to the loss of endothelium, myosin expression was reduced to sites of injury and showed no significant change with increasing cyclic pressure. A biaxial strain device may be employed to maintain the suitable mechanical force required to keep the endothelium intact. Further study is necessary to elucidate the biochemical pathways involved in differentiation and possible redifferentiation of myosin within the aortic valve.

Summary

A cyclic pressure bioreactor was created to compare the α/β-myosin heavy chain expression of porcine aortic heart valves between physiological and pathological conditions. The bioreactor was successful in meeting all system requirements and was therefore able to create a suitable environment for subsequent testing. Immunohistochemistry staining showed that myosin was expressed on the fibrosal endothelium and also illuminated smooth muscle cells within the subendothelial space. Cyclic pressure, however, was unable to maintain the endothelial layer, and myosin expression diminished over time. Leaflets tested within the bioreactor expressed myosin only at areas of high shear stress, such as sites of excision or tweezer penetration.

BIBLIOGRAPHY

1. Mehra R. Global public health problem of sudden cardiac death. J.Electrocardiol. 2007 Nov;40(6 Suppl):S118-S122.

2. Rosamond W, Flegal K, Furie K, Go A, Greenlund K, Haase N, Hailpern SM, Ho M, Howard V, Kissela B, et al. Heart disease and stroke statistics--2008 update: a report from the American Heart Association Statistics Committee and Stroke Statistics Subcommittee. Circulation 2008 Jan 29;117(4):e25-146.

3. Hall RJ. Aortic valve disease. Eur.Heart J. 1984 Mar;5 Suppl A:135-9.

4. Baxley WA. Aortic valve disease. Curr.Opin.Cardiol. 1994 Mar;9(2):152-7.

5. Leggett M, Otto CM. Aortic valve disease. Curr.Opin.Cardiol. 1996 Mar;11(2):120-5.

6. Rosamond W, Flegal K, Friday G, Furie K, Go A, Greenlund K, Haase N, Ho M, Howard V, Kissela B, et al. Heart disease and stroke statistics--2007 update: a report from the American Heart Association Statistics Committee and Stroke Statistics Subcommittee. Circulation 2007 Feb 6;115(5):e69-171.

7. Bhatia A, Vesely I. The effect of glycosaminoglycans and hydration on the viscoelastic properties of aortic valve cusps. Conf.Proc.IEEE Eng Med.Biol.Soc. 2005;3:2979-80.

8. Yacoub MH, Cohn LH. Novel approaches to cardiac valve repair: from structure to function: Part I. Circulation 2004 Mar 2;109(8):942-50.

9. Rabkin E, Aikawa M, Stone JR, Fukumoto Y, Libby P, Schoen FJ. Activated interstitial myofibroblasts express catabolic enzymes and mediate matrix remodeling in myxomatous heart valves. Circulation 2001 Nov 20;104(21):2525-32.

10. Deck JD, Thubrikar MJ, Schneider PJ, Nolan SP. Structure, stress, and tissue repair in aortic valve leaflets. Cardiovasc.Res. 1988 Jan;22(1):7-16.

11. Thubrikar M, Piepgrass WC, Shaner TW, Nolan SP. The design of the normal aortic valve. Am.J.Physiol 1981 Dec;241(6):H795-H801.

12. Doehring TC, Kahelin M, Vesely I. Mesostructures of the aortic valve. J.Heart Valve Dis. 2005 Sep;14(5):679-86.

13. Thubrikar M, Piepgrass WC, Bosher LP, Nolan SP. The elastic modulus of canine aortic valve leaflets in vivo and in vitro. Circ.Res. 1980 Nov;47(5):792-800.

14. Thubrikar MJ, Aouad J, Nolan SP. Comparison of the in vivo and in vitro mechanical properties of aortic valve leaflets. J.Thorac.Cardiovasc.Surg. 1986 Jul;92(1):29-36.

15. Stella JA, Sacks MS. On the biaxial mechanical properties of the layers of the aortic valve leaflet. J.Biomech.Eng 2007 Oct;129(5):757-66.

16. Scott MJ, Vesely I. Morphology of porcine aortic valve cusp elastin. J.Heart Valve Dis. 1996 Sep;5(5):464-71.

17. Markwald RR, Fitzharris TP, Manasek FJ. Structural development of endocardial cushions. Am.J.Anat. 1977 Jan;148(1):85-119.

18. Butcher JT, Markwald RR. Valvulogenesis: the moving target. Philos.Trans.R.Soc.Lond B Biol.Sci. 2007 Aug 29;362(1484):1489-503.

19. Butcher JT, Norris RA, Hoffman S, Mjaatvedt CH, Markwald RR. Periostin promotes atrioventricular mesenchyme matrix invasion and remodeling mediated by integrin signaling through Rho/PI 3-kinase. Dev.Biol. 2007 Feb 1;302(1):256-66.

20. Delot EC. Control of endocardial cushion and cardiac valve maturation by BMP signaling pathways. Mol.Genet.Metab 2003 Sep;80(1-2):27-35.

21. Jiao K, Kulessa H, Tompkins K, Zhou Y, Batts L, Baldwin HS, Hogan BL. An essential role of Bmp4 in the atrioventricular septation of the mouse heart. Genes Dev. 2003 Oct 1;17(19):2362-7.

22. Norris RA, Moreno-Rodriguez RA, Sugi Y, Hoffman S, Amos J, Hart MM, Potts JD, Goodwin RL, Markwald RR. Periostin regulates atrioventricular valve maturation. Dev.Biol. 2008 Apr 15;316(2):200-13.

23. Lincoln J, Alfieri CM, Yutzey KE. BMP and FGF regulatory pathways control cell lineage diversification of heart valve precursor cells. Dev.Biol. 2006 Apr 15;292(2):292-302.

24. Lincoln J, Lange AW, Yutzey KE. Hearts and bones: shared regulatory mechanisms in heart valve, cartilage, tendon, and bone development. Dev.Biol. 2006 Jun 15;294(2):292-302.

25. Deck JD. Endothelial cell orientation on aortic valve leaflets. Cardiovasc.Res. 1986 Oct;20(10):760-7.

26. Butcher JT, Simmons CA, Warnock JN. Mechanobiology of the aortic heart valve. J.Heart Valve Dis. 2008 Jan;17(1):62-73.

27. Mohler ER, III. Mechanisms of aortic valve calcification. Am.J.Cardiol. 2004 Dec 1;94(11):1396-402, A6.

28. Butcher JT, Penrod AM, Garcia AJ, Nerem RM. Unique morphology and focal adhesion development of valvular endothelial cells in static and fluid flow environments. Arterioscler.Thromb.Vasc.Biol. 2004 Aug;24(8):1429-34.

29. Butcher JT, Tressel S, Johnson T, Turner D, Sorescu G, Jo H, Nerem RM. Transcriptional profiles of valvular and vascular endothelial cells reveal phenotypic differences: influence of shear stress. Arterioscler.Thromb.Vasc.Biol. 2006 Jan;26(1):69-77.

30. Simmons CA, Zilberberg J, Davies PF. A rapid, reliable method to isolate high quality endothelial RNA from small spatially-defined locations. Ann.Biomed.Eng 2004 Oct;32(10):1453-9.

31. Durbin AD, Gotlieb AI. Advances towards understanding heart valve response to injury. Cardiovasc.Pathol. 2002 Mar;11(2):69-77.

32. Mulholland DL, Gotlieb AI. Cell biology of valvular interstitial cells. Can.J.Cardiol. 1996 Mar;12(3):231-6.

33. Latif N, Sarathchandra P, Thomas PS, Antoniw J, Batten P, Chester AH, Taylor PM, Yacoub MH. Characterization of structural and signaling molecules by human valve interstitial cells and comparison to human mesenchymal stem cells. J.Heart Valve Dis. 2007 Jan;16(1):56-66.

34. Rabkin-Aikawa E, Farber M, Aikawa M, Schoen FJ. Dynamic and reversible changes of interstitial cell phenotype during remodeling of cardiac valves. J.Heart Valve Dis. 2004 Sep;13(5):841-7.

35. Segura AM, Luna RE, Horiba K, Stetler-Stevenson WG, McAllister HA, Jr., Willerson JT, Ferrans VJ. Immunohistochemistry of matrix metalloproteinases and their inhibitors in thoracic aortic aneurysms and

aortic valves of patients with Marfan's syndrome. Circulation 1998 Nov 10;98(19 Suppl):II331-II337.

36. Narine K, DeWever O, Cathenis K, Mareel M, Van BY, Van NG. Transforming growth factor-beta-induced transition of fibroblasts: a model for myofibroblast procurement in tissue valve engineering. J.Heart Valve Dis. 2004 Mar;13(2):281-9.

37. Messier RH, Jr., Bass BL, Aly HM, Jones JL, Domkowski PW, Wallace RB, Hopkins RA. Dual structural and functional phenotypes of the porcine aortic valve interstitial population: characteristics of the leaflet myofibroblast. J.Surg.Res. 1994 Jul;57(1):1-21.

38. Roy A, Brand NJ, Yacoub MH. Molecular characterization of interstitial cells isolated from human heart valves. J.Heart Valve Dis. 2000 May;9(3):459-64.

39. Bairati A, DeBiasi S. Presence of a smooth muscle system in aortic valve leaflets. Anat.Embryol.(Berl) 1981;161(3):329-40.

40. Rabkin E, Hoerstrup SP, Aikawa M, Mayer JE, Jr., Schoen FJ. Evolution of cell phenotype and extracellular matrix in tissue-engineered heart valves during in-vitro maturation and in-vivo remodeling. J.Heart Valve Dis. 2002 May;11(3):308-14.

41. Merryman WD, Youn I, Lukoff HD, Krueger PM, Guilak F, Hopkins RA, Sacks MS. Correlation between heart valve interstitial cell stiffness and transvalvular pressure: implications for collagen biosynthesis. Am.J.Physiol Heart Circ.Physiol 2006 Jan;290(1):H224-H231.

42. Goodwin RL, Nesbitt T, Price RL, Wells JC, Yost MJ, Potts JD. Three-dimensional model system of valvulogenesis. Dev.Dyn. 2005 May;233(1):122-9.

43. Garcia-Martinez V, Hurle JM. Cell shape and cytoskeletal organization of the endothelial cells of the semilunar heart valves in the developing chick. Anat.Embryol.(Berl) 1986;174(1):83-9.

44. Bannykh S, Mironov A, Jr., Bannykh G, Mironov A. The morphology of valves and valve-like structures in the canine and feline thoracic duct. Anat.Embryol.(Berl) 1995 Sep;192(3):265-74.

45. Fae KC, efenbach da SD, Bilate AM, Tanaka AC, Pomerantzeff PM, Kiss MH, Silva CA, Cunha-Neto E, Kalil J, Guilherme L. PDIA3, HSPA5 and vimentin, proteins identified by 2-DE in the valvular tissue, are the target

antigens of peripheral and heart infiltrating T cells from chronic rheumatic heart disease patients. J.Autoimmun. 2008 Jun 7.

46. Hoh JF, McGrath PA, Hale PT. Electrophoretic analysis of multiple forms of rat cardiac myosin: effects of hypophysectomy and thyroxine replacement. J.Mol.Cell Cardiol. 1978 Nov;10(11):1053-76.

47. Lompre AM, Nadal-Ginard B, Mahdavi V. Expression of the cardiac ventricular alpha- and beta-myosin heavy chain genes is developmentally and hormonally regulated. J.Biol.Chem. 1984 May 25;259(10):6437-46.

48. Yamauchi-Takihara K, Sole MJ, Liew J, Ing D, Liew CC. Characterization of human cardiac myosin heavy chain genes. Proc.Natl.Acad.Sci.U.S.A 1989 May;86(10):3504-8.

49. Goldspink P, Sharp W, Russell B. Localization of cardiac (alpha)-myosin heavy chain mRNA is regulated by its 3' untranslated region via mechanical activity and translational block. J.Cell Sci. 1997 Dec;110 (Pt 23):2969-78.

50. Shyu KG, Chen JJ, Shih NL, Wang DL, Chang H, Lien WP, Liew CC. Regulation of human cardiac myosin heavy chain genes by cyclical mechanical stretch in cultured cardiocytes. Biochem.Biophys.Res.Commun. 1995 May 16;210(2):567-73.

51. Miyata S, Minobe W, Bristow MR, Leinwand LA. Myosin heavy chain isoform expression in the failing and nonfailing human heart. Circ.Res. 2000 Mar 3;86(4):386-90.

52. Caforio AL, Grazzini M, Mann JM, Keeling PJ, Bottazzo GF, McKenna WJ, Schiaffino S. Identification of alpha- and beta-cardiac myosin heavy chain isoforms as major autoantigens in dilated cardiomyopathy. Circulation 1992 May;85(5):1734-42.

53. Rabkin SW. The association of hypertension and aortic valve sclerosis. Blood Press 2005;14(5):264-72.

54. Schoen FJ. Aortic valve structure-function correlations: role of elastic fibers no longer a stretch of the imagination. J.Heart Valve Dis. 1997 Jan;6(1):1-6.

55. Vesely I. The role of elastin in aortic valve mechanics. J.Biomech. 1998 Feb;31(2):115-23.

56. Vesely I. Heart valve tissue engineering. Circ.Res. 2005 Oct 14;97(8):743-55.

57. Weinberg EJ, Kaazempur Mofrad MR. Transient, three-dimensional, multiscale simulations of the human aortic valve. Cardiovasc.Eng 2007 Dec;7(4):140-55.

58. Thubrikar MJ, Aouad J, Nolan SP. Comparison of the in vivo and in vitro mechanical properties of aortic valve leaflets. J.Thorac.Cardiovasc.Surg. 1986 Jul;92(1):29-36.

59. Freeman RV, Otto CM. Spectrum of calcific aortic valve disease: pathogenesis, disease progression, and treatment strategies. Circulation 2005 Jun 21;111(24):3316-26.

60. Robicsek F, Thubrikar MJ, Fokin AA. Cause of degenerative disease of the trileaflet aortic valve: review of subject and presentation of a new theory. Ann.Thorac.Surg. 2002 Apr;73(4):1346-54.

61. Thubrikar MJ, Aouad J, Nolan SP. Patterns of calcific deposits in operatively excised stenotic or purely regurgitant aortic valves and their relation to mechanical stress. Am.J.Cardiol. 1986 Aug 1;58(3):304-8.

62. O'Brien KD, Reichenbach DD, Marcovina SM, Kuusisto J, Alpers CE, Otto CM. Apolipoproteins B, (a), and E accumulate in the morphologically early lesion of 'degenerative' valvular aortic stenosis. Arterioscler.Thromb.Vasc.Biol. 1996 Apr;16(4):523-32.

63. Otto CM, Kuusisto J, Reichenbach DD, Gown AM, O'Brien KD. Characterization of the early lesion of 'degenerative' valvular aortic stenosis. Histological and immunohistochemical studies. Circulation 1994 Aug;90(2):844-53.

64. Pickering TG, James GD. Ambulatory blood pressure and prognosis. J.Hypertens.Suppl 1994 Nov;12(8):S29-S33.

65. Oparil S. Pathogenesis of ventricular hypertrophy. J.Am.Coll.Cardiol. 1985 Jun;5(6 Suppl):57B-65B.

66. Dzau VJ. Cell biology and genetics of angiotensin in cardiovascular disease. J.Hypertens.Suppl 1994 Jul;12(4):S3-10.

67. Dzau VJ, Gibbons GH, Morishita R, Pratt RE. New perspectives in hypertension research. Potentials of vascular biology. Hypertension 1994 Jun;23(6 Pt 2):1132-40.

68. Badoual T, Monin JL. [Aortic stenosis]. Rev.Prat. 2006 Dec 15;56(19):2173-8.

69. Bekeredjian R, Grayburn PA. Valvular heart disease: aortic regurgitation. Circulation 2005 Jul 5;112(1):125-34.

70. Carabello BA, Crawford FA, Jr. Valvular heart disease. N.Engl.J.Med. 1997 Jul 3;337(1):32-41.

71. Delaye J, Chevalier P, Delahaye F, Didier B. Valvular aortic stenosis and coronary atherosclerosis: pathophysiology and clinical consequences. Eur.Heart J. 1988 Apr;9 Suppl E:83-6.

72. Thubrikar M, Nolan SP, Bosher LP, Deck JD. The cyclic changes and structure of the base of the aortic valve. Am.Heart J. 1980 Feb;99(2):217-24.

73. Zezulka A, Mackinnon J, Beevers DG. Hypertension in aortic valve disease and its response to valve replacement. Postgrad.Med.J. 1992 Mar;68(797):180-5.

74. Nishimura RA. Cardiology patient pages. Aortic valve disease. Circulation 2002 Aug 13;106(7):770-2.

75. Nishimura RA, McGoon MD, Schaff HV, Giuliani ER. Chronic aortic regurgitation: indications for operation--1988. Mayo Clin.Proc. 1988 Mar;63(3):270-80.

76. Hammermeister K, Sethi GK, Henderson WG, Grover FL, Oprian C, Rahimtoola SH. Outcomes 15 years after valve replacement with a mechanical versus a bioprosthetic valve: final report of the Veterans Affairs randomized trial. J.Am.Coll.Cardiol. 2000 Oct;36(4):1152-8.

77. Khan SS, Trento A, DeRobertis M, Kass RM, Sandhu M, Czer LS, Blanche C, Raissi S, Fontana GP, Cheng W, et al. Twenty-year comparison of tissue and mechanical valve replacement. J.Thorac.Cardiovasc.Surg. 2001 Aug;122(2):257-69.

78. Langley SM, McGuirk SP, Chaudhry MA, Livesey SA, Ross JK, Monro JL. Twenty-year follow-up of aortic valve replacement with antibiotic sterilized homografts in 200 patients. Semin.Thorac.Cardiovasc.Surg. 1999 Oct;11(4 Suppl 1):28-34.

79. Lupinetti FM, Warner J, Jones TK, Herndon SP. Comparison of human tissues and mechanical prostheses for aortic valve replacement in children. Circulation 1997 Jul 1;96(1):321-5.

80. Schoen FJ, Collins JJ, Jr., Cohn LH. Long-term failure rate and morphologic correlations in porcine bioprosthetic heart valves. Am.J.Cardiol. 1983 Mar 15;51(6):957-64.

81. Takkenberg JJ, van Herwerden LA, Eijkemans MJ, Bekkers JA, Bogers AJ. Evolution of allograft aortic valve replacement over 13 years: results of 275 procedures. Eur.J.Cardiothorac.Surg. 2002 Apr;21(4):683-91.

82. Willems TP, Takkenberg JJ, Steyerberg EW, Kleyburg-Linkers VE, Roelandt JR, Bos E, van Herwerden LA. Human tissue valves in aortic position: determinants of reoperation and valve regurgitation. Circulation 2001 Mar 20;103(11):1515-21.

83. O'Brien MF, Stafford EG, Gardner MA, Pohlner PG, Tesar PJ, Cochrane AD, Mau TK, Gall KL, Smith SE. Allograft aortic valve replacement: long-term follow-up. Ann.Thorac.Surg. 1995 Aug;60(2 Suppl):S65-S70.

84. Palka P, Harrocks S, Lange A, Burstow DJ, O'Brien MF. Primary aortic valve replacement with cryopreserved aortic allograft: an echocardiographic follow-up study of 570 patients. Circulation 2002 Jan 1;105(1):61-6.

85. Carpentier A. From valvular xenograft to valvular bioprosthesis (1965-1977). Med.Instrum. 1977 Mar;11(2):98-101.

86. Carpentier A, Deloche A, Relland J, Fabiani JN, Forman J, Camilleri JP, Soyer R, Dubost C. Six-year follow-up of glutaraldehyde-preserved heterografts. With particular reference to the treatment of congenital valve malformations. J.Thorac.Cardiovasc.Surg. 1974 Nov;68(5):771-82.

87. Sacks MS, Schoen FJ. Collagen fiber disruption occurs independent of calcification in clinically explanted bioprosthetic heart valves. J.Biomed.Mater.Res. 2002 Dec 5;62(3):359-71.

88. David TE, Gott VL, Harker LA, Miller GE, Jr., Naftel DC, Turpie AG. Mechanical valves. Ann.Thorac.Surg. 1996 Nov;62(5):1567-70.

89. Travis BR, Heinrich RS, Ensley AE, Gibson DE, Hashim S, Yoganathan AP. The hemodynamic effects of mechanical prosthetic valve type and orientation on fluid mechanical energy loss and pressure drop in in vitro models of ventricular hypertrophy. J.Heart Valve Dis. 1998 May;7(3):345-54.

90. Yoganathan AP, Woo YR, Sung HW, Jones M. Advances in prosthetic heart valves: fluid mechanics of aortic valve designs. J.Biomater.Appl. 1988 Apr;2(4):579-614.

91. Yoganathan AP, He Z, Casey JS. Fluid mechanics of heart valves. Annu.Rev.Biomed.Eng 2004;6:331-62.

92. Gott VL, Alejo DE, Cameron DE. Mechanical heart valves: 50 years of evolution. Ann.Thorac.Surg. 2003 Dec;76(6):S2230-S2239.

93. Black MM, Drury PJ, Tindale WB. Twenty-five years of heart valve substitutes: a review. J.R.Soc.Med. 1983 Aug;76(8):667-80.

94. Hammermeister K, Sethi GK, Henderson WG, Grover FL, Oprian C, Rahimtoola SH. Outcomes 15 years after valve replacement with a mechanical versus a bioprosthetic valve: final report of the Veterans Affairs randomized trial. J.Am.Coll.Cardiol. 2000 Oct;36(4):1152-8.

95. Stock UA, Vacanti JP, Mayer Jr JE, Wahlers T. Tissue engineering of heart valves -- current aspects. Thorac.Cardiovasc.Surg. 2002 Jun;50(3):184-93.

96. Sodian R, Sperling JS, Martin DP, Egozy A, Stock U, Mayer JE, Jr., Vacanti JP. Fabrication of a trileaflet heart valve scaffold from a polyhydroxyalkanoate biopolyester for use in tissue engineering. Tissue Eng 2000 Apr;6(2):183-8.

97. Gunatillake P, Mayadunne R, Adhikari R. Recent developments in biodegradable synthetic polymers. Biotechnol.Annu.Rev. 2006;12:301-47.

98. Gunatillake PA, Adhikari R. Biodegradable synthetic polymers for tissue engineering. Eur.Cell Mater. 2003 May 20;5:1-16.

99. Jockenhoevel S, Zund G, Hoerstrup SP, Chalabi K, Sachweh JS, Demircan L, Messmer BJ, Turina M. Fibrin gel -- advantages of a new scaffold in cardiovascular tissue engineering. Eur.J.Cardiothorac.Surg. 2001 Apr;19(4):424-30.

100. Mol A, van Lieshout MI, Dam-de Veen CG, Neuenschwander S, Hoerstrup SP, Baaijens FP, Bouten CV. Fibrin as a cell carrier in cardiovascular tissue engineering applications. Biomaterials 2005 Jun;26(16):3113-21.

101. Ye Q, Zund G, Benedikt P, Jockenhoevel S, Hoerstrup SP, Sakyama S, Hubbell JA, Turina M. Fibrin gel as a three dimensional matrix in cardiovascular tissue engineering. Eur.J.Cardiothorac.Surg. 2000 May;17(5):587-91.

102. Seliktar D, Nerem RM, Galis ZS. The role of matrix metalloproteinase-2 in the remodeling of cell-seeded vascular constructs subjected to cyclic strain. Ann.Biomed.Eng 2001 Nov;29(11):923-34.

103. Shin HY, Bizios R, Gerritsen ME. Cyclic pressure modulates endothelial barrier function. Endothelium 2003;10(3):179-87.

104. Hoerstrup SP, Sodian R, Sperling JS, Vacanti JP, Mayer JE, Jr. New pulsatile bioreactor for in vitro formation of tissue engineered heart valves. Tissue Eng 2000 Feb;6(1):75-9.

105. Zeltinger J, Landeen LK, Alexander HG, Kidd ID, Sibanda B. Development and characterization of tissue-engineered aortic valves. Tissue Eng 2001 Feb;7(1):9-22.

106. Weston MW, Yoganathan AP. Biosynthetic activity in heart valve leaflets in response to in vitro flow environments. Ann.Biomed.Eng 2001 Sep;29(9):752-63.

107. Engelmayr GC, Jr., Hildebrand DK, Sutherland FW, Mayer JE, Jr., Sacks MS. A novel bioreactor for the dynamic flexural stimulation of tissue engineered heart valve biomaterials. Biomaterials 2003 Jun;24(14):2523-32.

108. Johnson DM, Chwirut DJ, Regnault WF. FDA's requirements for in-vitro performance data for prosthetic heart valves. J.Heart Valve Dis. 1994 May;3(3):228-34.

109. Jockenhoevel S, Zund G, Hoerstrup SP, Schnell A, Turina M. Cardiovascular tissue engineering: a new laminar flow chamber for in vitro improvement of mechanical tissue properties. ASAIO J. 2002 Jan;48(1):8-11.

110. Kim BS, Mooney DJ. Scaffolds for engineering smooth muscle under cyclic mechanical strain conditions. J.Biomech.Eng 2000 Jun;122(3):210-5.

111. Hildebrand DK, Wu ZJ, Mayer JE, Jr., Sacks MS. Design and hydrodynamic evaluation of a novel pulsatile bioreactor for biologically active heart valves. Ann.Biomed.Eng 2004 Aug;32(8):1039-49.

112. Reul H, Giersiepen M, Knott E. Laboratory testing of prosthetic heart valves. Eng Med. 1987 Apr;16(2):67-76.

113. Reul H, van Son JA, Steinseifer U, Schmitz B, Schmidt A, Schmitz C, Rau G. In vitro comparison of bileaflet aortic heart valve prostheses. St. Jude Medical, CarboMedics, modified Edwards-Duromedics, and Sorin-Bicarbon valves. J.Thorac.Cardiovasc.Surg. 1993 Sep;106(3):412-20.

114. Schichl K, Affeld K. A computer controlled versatile pulse duplicator for precision testing of artificial heart valves. Int.J.Artif.Organs 1993 Oct;16(10):722-8.

115. Warnock JN, Konduri S, He Z, Yoganathan AP. Design of a sterile organ culture system for the ex vivo study of aortic heart valves. J.Biomech.Eng 2005 Oct;127(5):857-61.

116. Xing Y, Warnock JN, He Z, Hilbert SL, Yoganathan AP. Cyclic pressure affects the biological properties of porcine aortic valve leaflets in a magnitude and frequency dependent manner. Ann.Biomed.Eng 2004 Nov;32(11):1461-70.

117. Barron V, Lyons E, Stenson-Cox C, McHugh PE, Pandit A. Bioreactors for cardiovascular cell and tissue growth: a review. Ann.Biomed.Eng 2003 Oct;31(9):1017-30.

118. Brathwaite D, Weissman C. The new onset of atrial arrhythmias following major noncardiothoracic surgery is associated with increased mortality. Chest 1998 Aug;114(2):462-8.

119. Walsh SR, Tang T, Gaunt ME, Schneider HJ. New arrhythmias after non-cardiothoracic surgery. BMJ 2006 Oct 7;333(7571):715.

120. Walsh SR, Oates JE, Anderson JA, Blair SD, Makin CA, Walsh CJ. Postoperative arrhythmias in colorectal surgical patients: incidence and clinical correlates. Colorectal Dis. 2006 Mar;8(3):212-6.

121. Walsh SR, Tang T, Wijewardena C, Yarham SI, Boyle JR, Gaunt ME. Postoperative arrhythmias in general surgical patients. Ann.R.Coll.Surg.Engl. 2007 Mar;89(2):91-5.

122. Aikawa M, Sivam PN, Kuro-o M, Kimura K, Nakahara K, Takewaki S, Ueda M, Yamaguchi H, Yazaki Y, Periasamy M, et al. Human smooth muscle myosin heavy chain isoforms as molecular markers for vascular development and atherosclerosis. Circ.Res. 1993 Dec;73(6):1000-12.

123. Izumo S, Lompre AM, Matsuoka R, Koren G, Schwartz K, Nadal-Ginard B, Mahdavi V. Myosin heavy chain messenger RNA and protein isoform transitions during cardiac hypertrophy. Interaction between hemodynamic and thyroid hormone-induced signals. J.Clin.Invest 1987 Mar;79(3):970-7.

124. Metzler S. Cyclic Strain Regulates Pro-Inflammatory Protein Expression in Porcine Aortic Valve Endothelial Cells. J.Heart Valve Dis. 2008.

125. Armstrong EJ, Bischoff J. Heart valve development: endothelial cell signaling and differentiation. Circ.Res. 2004 Sep 3;95(5):459-70.

126. Person AD, Klewer SE, Runyan RB. Cell biology of cardiac cushion development. Int.Rev.Cytol. 2005;243:287-335.

127. Ji X, Chen D, Xu C, Harris SE, Mundy GR, Yoneda T. Patterns of gene expression associated with BMP-2-induced osteoblast and adipocyte differentiation of mesenchymal progenitor cell 3T3-F442A. J.Bone Miner.Metab 2000;18(3):132-9.

APPENDIX A

SOLIDWORKS DRAWINGS OF BIOREACTOR

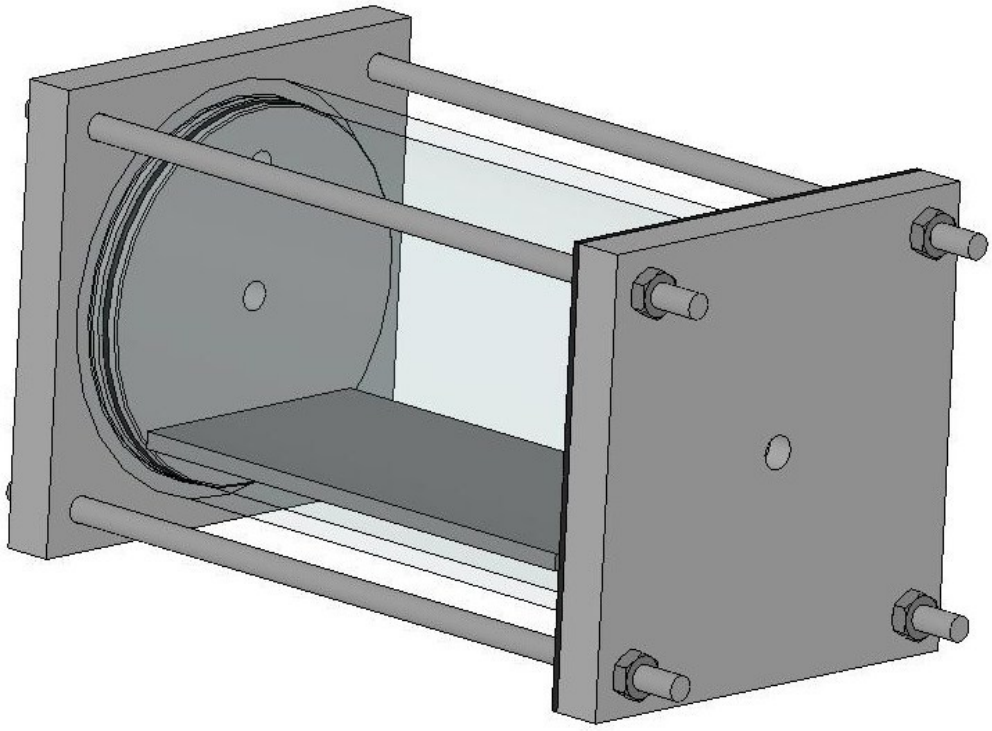

Isometric View of Bioreactor with Material Properties

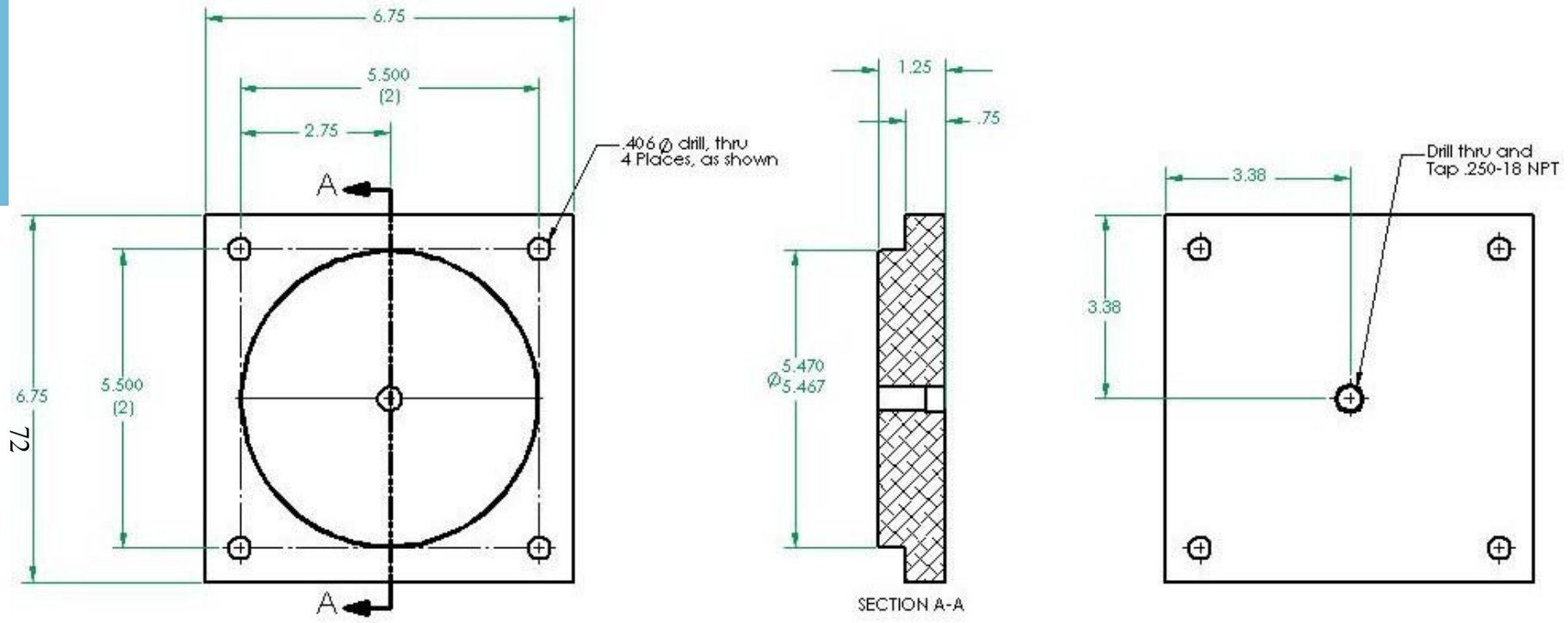

Dimensions of Front End Plate

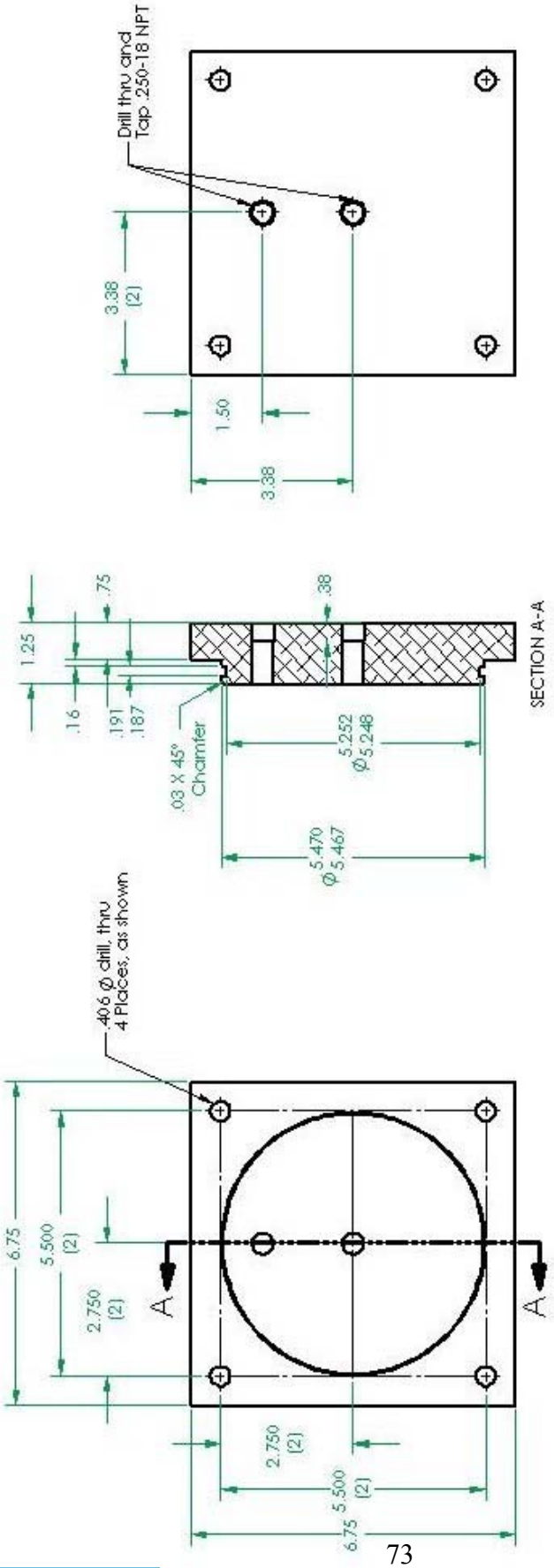

Dimensions of Rear End Plate

Dimensions of Acrylic Cylinder

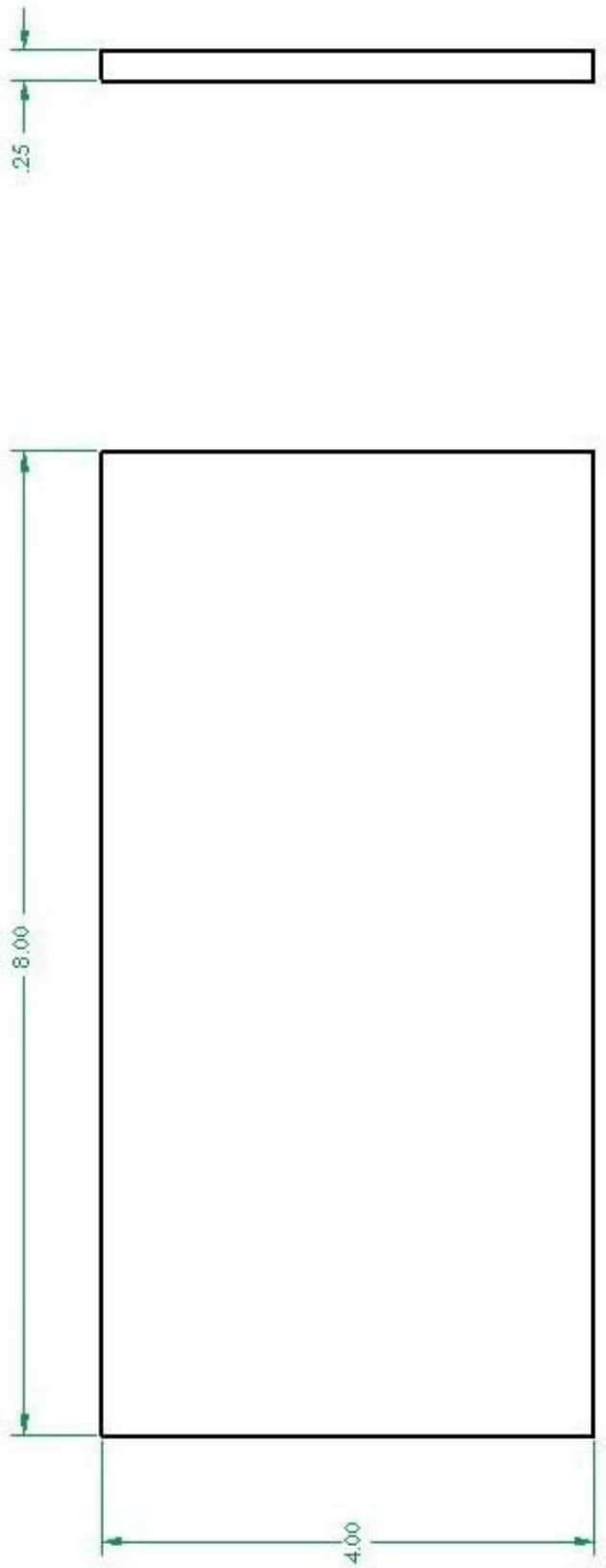

Dimensions of Sample Plate

Dissected Side View of Bioreactor

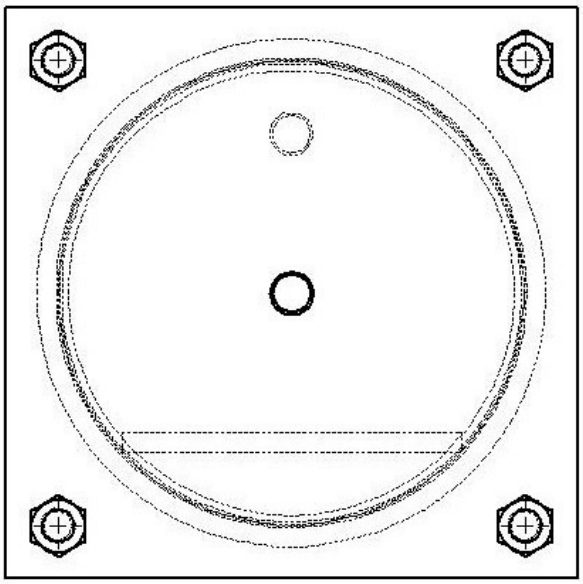

Front View of Bioreactor

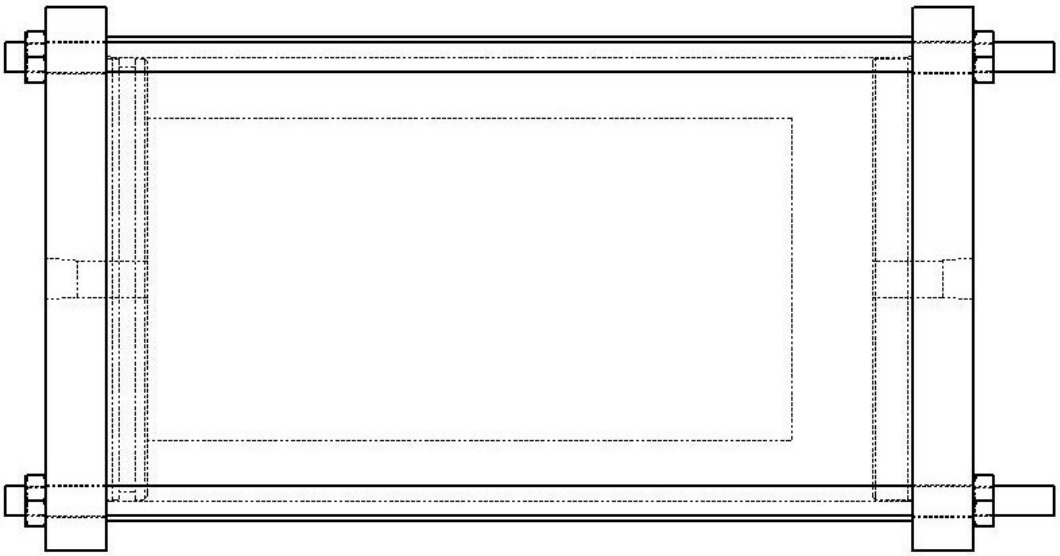

Top View of Bioreactor

APPENDIX B

ACTUAL PHOTOGRAPHS OF PRESSURE CHAMBER SYSTEM

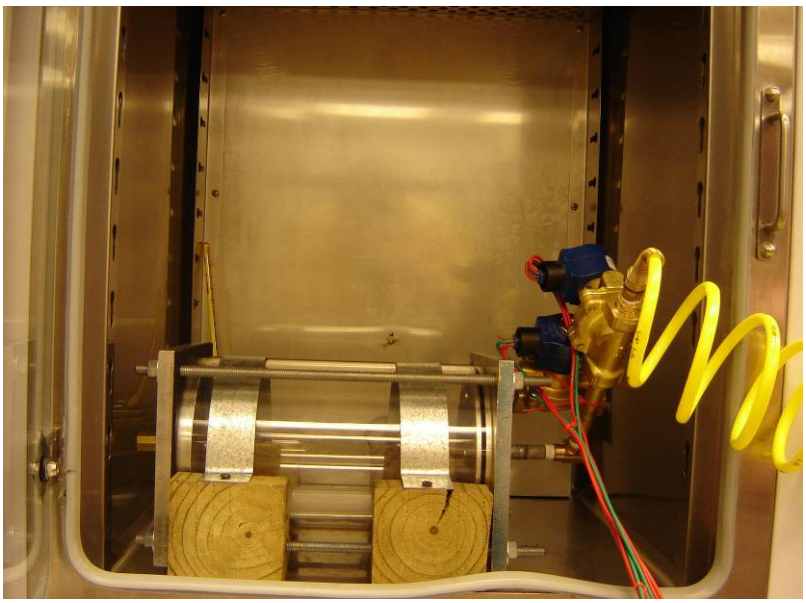

Bioreactor within Incubator

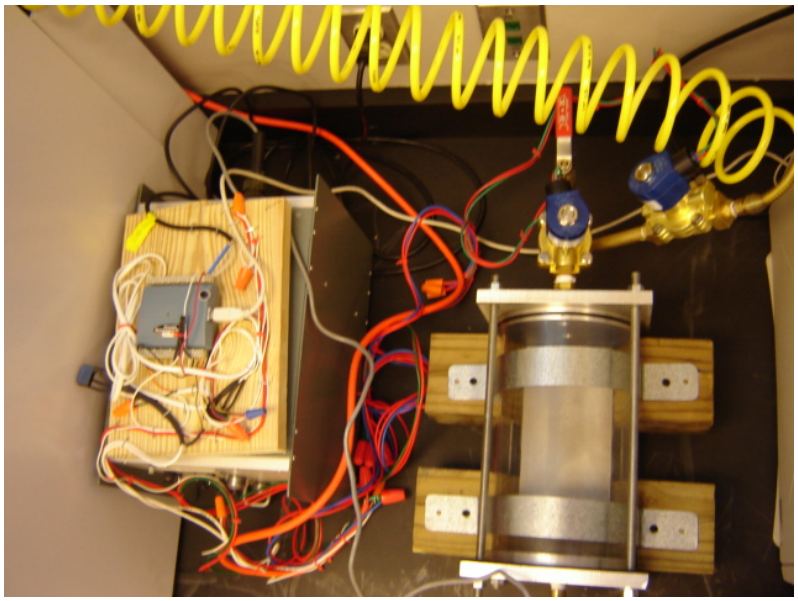

Top View of Bioreactor with Circuit Board

APPENDIX C

SCHEMATIC DRAWING OF ELECTRICAL CIRCUITRY

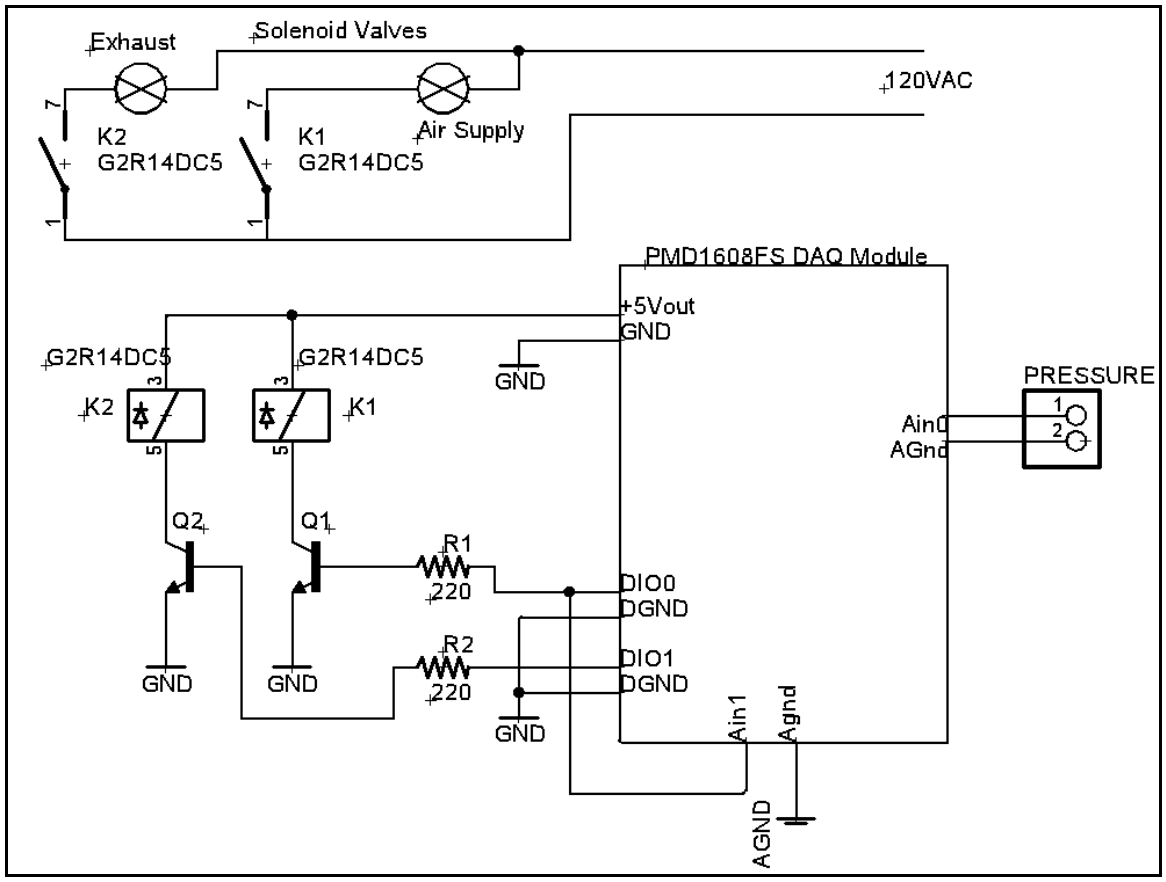

APPENDIX D

LABVIEW USER INTERFACE

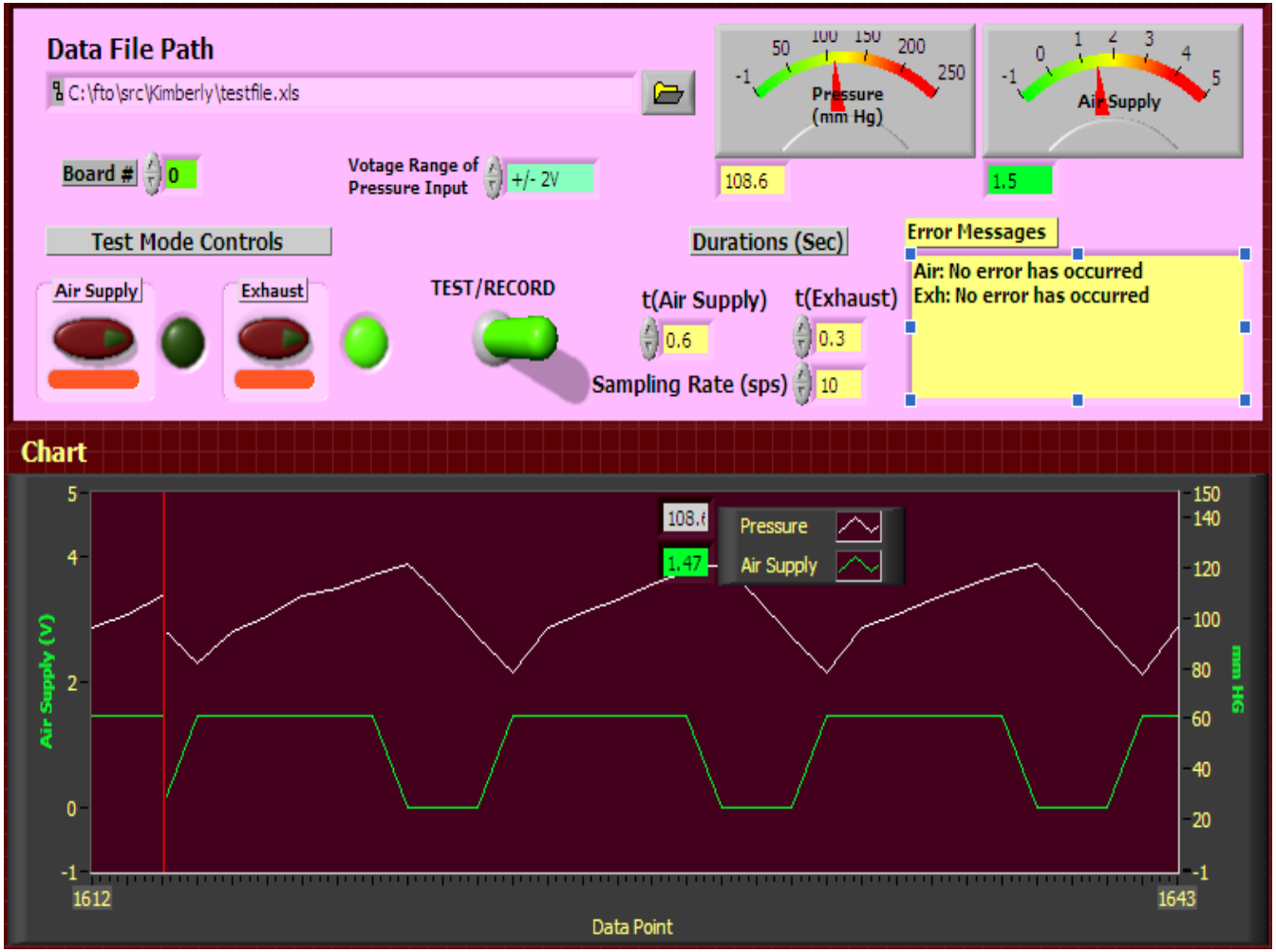

APPENDIX E

PROTOCOLS

Aortic Valve Leaflet Extraction and Culture

1. Extract aortic leaflets from annulus.

2. Place leaflets in Dulbecco's phosphate-buffer saline (PBS; Sigma, St. Louis, MO, USA).

3. Place leaflets in 6 well plates with 5 ml of media in each well.

Media:
Dulbecco's Modified Eagle Medium (DMEM; Sigma)
10% fetal bovine serum (Mediatech Inc., Herndon, VA, USA)
1% Anti-biotic/Anti-mycotic solution (Sigma)

4. Place leaflets in media in humidified incubator at 37˚C with 5% CO_2 for 24 hours.

5. Leaflets are prepared for pressurization.

Immunohistochemisty Protocol for TRS/Proteinase K Pretreatments

1. Prepare worksheet - List antibodies (Ab), number of slides for each with dilutions, pretreatments and reagent dispense locations and drop zones.

2. Program computer.

3. Prepare all reagents – Ab dilutions (α/β-myosin 1:800), blocking reagents, secondary and tertiary reagents, substrate and counterstain.

4. Number slides and label with Accession number, treatment identification and date. Use pencil.

5. Bake slides for 20 minutes at 60˚C.

6. Verify which slides require pretreatment with steam/TRS.

7. Set up steamer by filling bottom 2/3 full with dH_2O.

8. Fill slide container with appropriate amount of 1X TRS (approx. 200 ml).

9. Preheat steamer for 20 minutes.

10. Deparaffinization schedule:

    (Note: Deparaffinize slides to be pretreated with TRS first, then process others.)

    1. Xylene (used $\leq$ 3x) 10 min.
    2. Xylene (fresh) 10 min.
    3. 100% EtOH (used $\leq$ 3x) 10 dips
    4. 100% EtOH (fresh) 10 dips
    5. 70% EtOH (used $\leq$ 3x) 10 dips
    6. 70% EtOH (fresh) 10 dips
    7. Rinse well with dH_2O

11. Place slides in TBSTw for at least 5 min. (can be held o/n)

12. Place appropriate slides in steamer for 20 min. (hold others in TBSTw). When finished, let slides cool to room temp before putting in TBSTw for at least 5 min.

13. While steaming slides, saturate the autostainer with heated dH_2O.

14. Load slides.

15. Prime pumps.

16. Start run. Observe beginning of run to assure no problems.

17. Save run log.

18. Remove slides and rinse with dH_2O.

19. Load slides.

20. Prime pumps.

21. Start run. Observe beginning of run to assure no problems.

22. Save run log.

23. Remove slides and rinse with dH_2O.

24. Put slides in 100% EtOH for approximately 3 min and then into Clear-Rite.

25. Cover slip with Permount.